ONO DONORS
Chapter -3: Synthesis, Characterization, crystal structure and DNA binding behavior of ONO donor Schiff bases and their metal complexes

3.1 INTRODUCTION

Acyl-pyrazolones are good examples of heterocyclic β-diketonesand their analogues are good chelating agents for different metal ions. They form many coordination compounds that have wide range of applications in several domains [240-243]. They are employed as catalysts [244,245] and are potential anti-tumorals [246]. Pyrazolone-5 derivatives such as antipyrine and amido-pyrine are well known analgesics and are widely used in medicine [247,248]. They are starting materials for the synthesis of biologically active compounds [249] and are used for the preparation of condensed heterocyclic systems [250]. Of particular importance is the existence of these compounds in different tautomeric forms such as CH, OH and NH. All these unique features of these compounds have attracted the researchers and it can be seen from the wide literature available in this field [252-254].

Research in the field of acyl pyrazolone based Schiff bases and their metal complexes are of current interest. Preparationand characterization of 4-acetyl-3 methly-1-(4-methyl phenyl)-2-pyrazolin-5-one and its Cu(II) complex have been reported in 2004 focusing on spectroscopic studies of the complex [255]. The new ligand was used in solvent extraction chemistry. The structure suggested for the Cu(II) is given below.

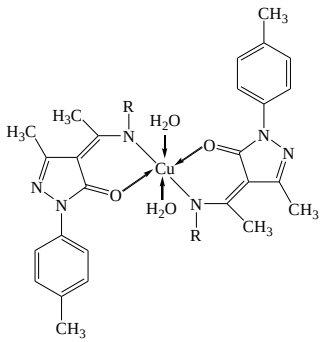

Vanadyl complexes have more applications now in biological systems because of their less toxicity compared to vanadate compounds. Synthesis and characterization of some pyrazolone analogues have been reported by Jadeja and Shah [256]. Vanadyl

complex of 4-benzoyl-3-methyl-1-(4-methyl phenyl)-2-pyrazoline-5-one is represented below:

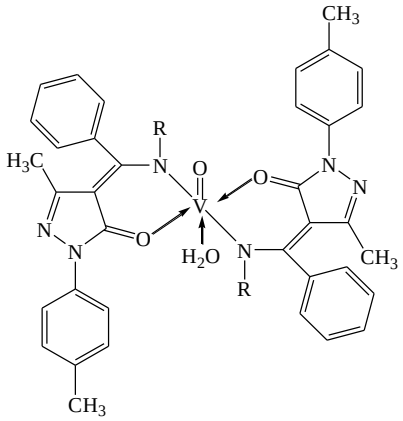

Parmar and Teraiya [257] have reported Co(II) and Ni(II) complexes of bis ketimino Schiff bases . The Schiff base has been prepared from 4-butyryl-3-methyl-1-phenyl-2-pyrazoline-5-one with o, m and p–phenylene diamine benzidine and ethylene diamine. The general representation is shown below:

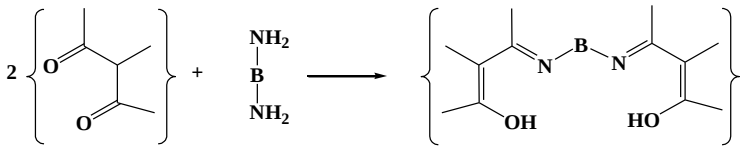

The pyrazolone based Schiff base is found in the following tautomeric forms:

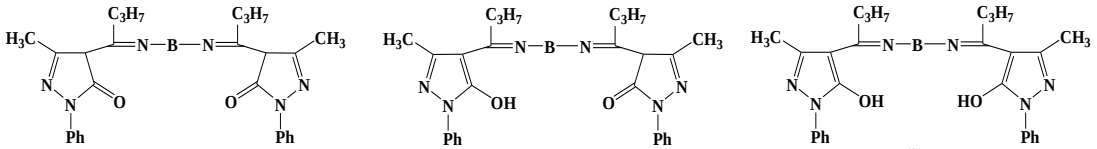

(1) (2) (3)

Analysis of Schiff bases showed 1:1 :: metal: ligand stoichiometry. The m or p phenelidine or benzidine Schiff base complexes were however found to be dimeric. The formation of the metal chelate can be represented by general formula.

$$nM(NO_3)_2.\,6H_2O + nH_2L \xrightarrow[\text{reflux}]{\text{Ethanol}} [ML(H_2O)_2]_n + 2nHNO_3 + 4nH_2O$$

where M=Co(II) or Ni(II) and n=1 for monomeric and 2 for dimeric complexes.

Suggested structure of the chelate of 1:1 metal:ligand complex is as follows.

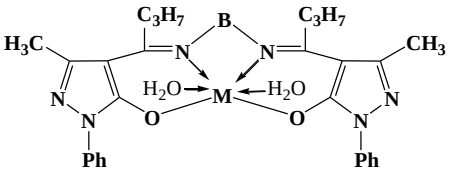

Suggested structure of the chelate of 2:2 metal:ligand complex stochiometry complex is given below;

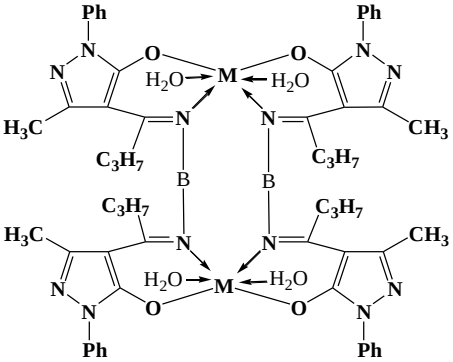

Oxovanadium(IV) complex of multidentate pyrazolone ligand was prepared and its catalytic property in the oxidation of styrene was studied[258]. The catalyst was used three times without any significant lose of catalytic activity. Oxovanidium complexes are of importance due to their biological activity, medicinal applications and catalytic property.

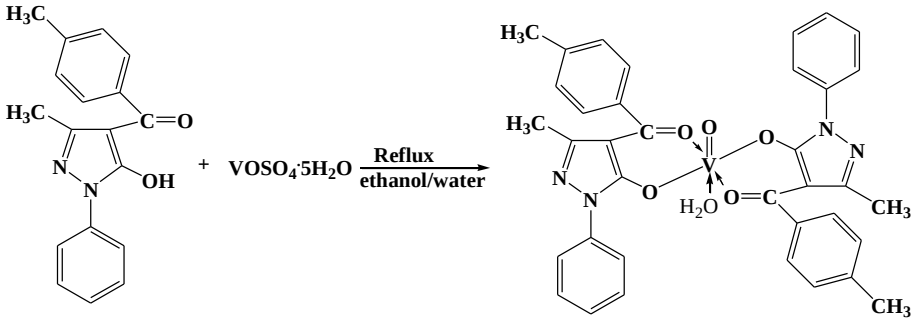

A binuclear Cu(II) complex $[Cu_2(L)_2]$ was prepared from tridentate Schiff base of 4-acyl/aryl pyrazolone with 2-amino phenol and the structure of the complex was proposed by Moorjani *et al.* [259] on the basis of elemental analysis and spectroscopic studies.

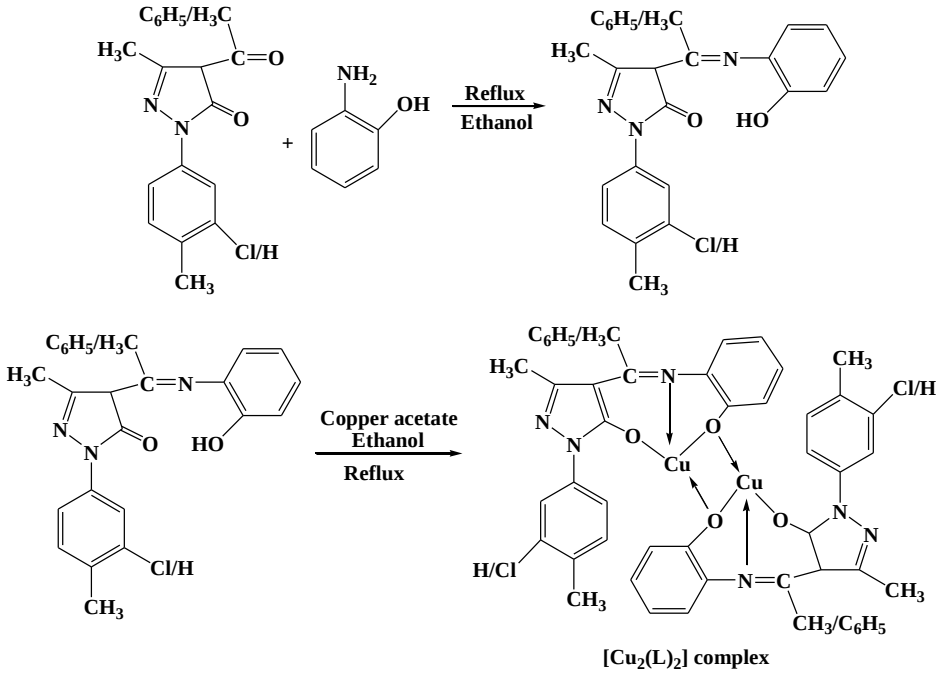

Jadeja *et al.*[260] have synthesized Zn-4-acyl-pyrazolone-1,10- phenanthroline complex, a complex with mixed ligands and studied its crystal structure and DNA binding behavior with the UV-Visible, Flourescense spectroscopy method and viscosity measurements.

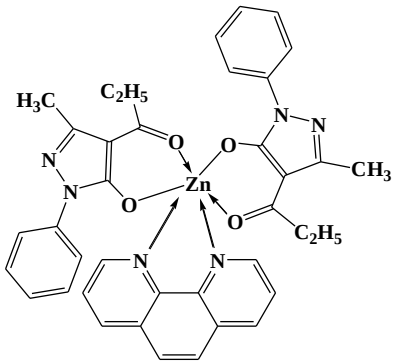

Jadeja *et al.* [261] carried out the synthesis and structural studies of a series of pyrazolone based Schiff base ligands and DNA binding studies of their Cu(II) complexes.

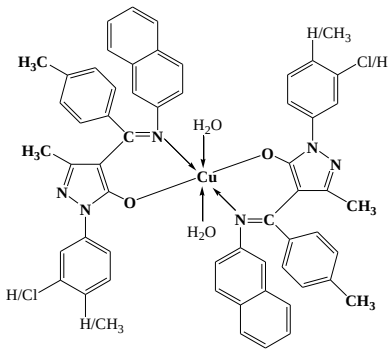

Vyas *et al.* [262] have synthesized a ternary Cu(II) complex from 4-toluoyl pyrazolone based thio-semicarbazone and 1,10-phenanthroline. The crystal structure of this kind of ternary complex, its DNA binding, protein binding and anti-cancerous activity against A549 lung cancer cells, have been reported for the first time.

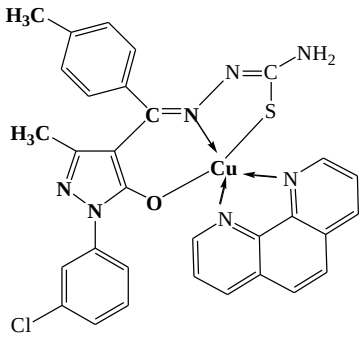

Against this background, a study of synthesis, characterization and DNA binding behavior of Cu(II) complex derived from 4-acyl-pyrazolone-ethanol amine Schiff base ONO donor ligandsisreported in the following chapter.

3.2 EXPERIMENTAL SECTION

3.2.1 Materials

The reagents and chemicals of analytical grade were procured from commercial sources.Solvents used for electrochemicalandspectroscopicstudieswerepurifiedusingstandardprocedures[151]. Disodium salt of calf thymus DNA (CT-DNA), purchased from Sigma, was stored at 4 °C and used as received. ThestocksolutionofDNAwaspreparedbydissolvingappropriateamountofDNAinH_2O and storedat4 ºC.Theratiooftheabsorbanceat260and280nm(A_{260}/A_{280})wascheckedtobe ~1.96,indicatingthattheDNAissufficientlyfreefromprotein[263]. TheconcentrationofDNA wasdeterminedspectrophotometricallyat260nmafter1:100dilutionusingtheknownmolar extinctioncoefficientvalueof670$M^{-1}cm^{-1}$[264]. Ethidium bromide(EB)wasobtainedfromHi-medialaboratoriesPvt.Ltd.,Mumbai.Double distilledwaterwasusedforpreparingallthesolutions.Purityoftheligandsanditscomplexes was evaluated bythin layer chromatography.

IR spectra (4000–400 cm^{-1}) of the ligands and metal complexes were recorded using KBr discs on 8400 FT-IR Shimadzu spectrometer. The mass spectra of the

ligands were recorded on a Trace GC ultra DSQ II. ^{1}H NMR spectra of ligands were recorded on Bruker Avance-II 400 MHz FT-NMR spectrometer using TMS as an internal standard and $CDCl_3$ as a solvent.X-ray intensity data were collected on Bruker CCD area-detector diffractometer equipped with graphite monochromated Mo Kα radiation (λ= 0.71073 Å). ESI-Mass spectra of complexes were recorded VG-70S spectrometer. Electronic spectra of the metal complexes in DMF were recorded on a Perkin-Elmer Lambda 19 spectrophotometer. Molar conductance of the metal complexes was determined on systronics direct reading conductivity meter type CM-82T. Elemental analysis (C, H and N) were carried out on elemental analyzer Perkin-Elmer 2400, while analysis of copper was determined by EDTA after decomposing the complexes with HNO_3. Magnetic susceptibility measurements of the complexes were carried out by Gouy balance using Hg $[Co(SCN)_4]$ as calibrant. Purity of the ligands and their complexes was evaluated by thin layer chromatography.

Synthesis of PMP, MCPMP and PTPMP

PMP (5-methyl-4-(4-methyl-benzoyl)-2-phenyl-2,4-dihydro-pyrazol-3-one), PTPMP (5-methyl-4-(4-methyl-benzoyl)-2-*p*-tolyl-2,4-dihydro-pyrazol-3-one) and MCPMP (2-(3-chloro-phenyl)-5-methyl-4-(4-methyl-benzoyl))-2,4-dihydro-pyrazol-3-one) were synthesized according to method reported. [265]

3.2.2 Single crystal X-ray structure determination

Single-crystal X-ray diffraction measurement for the Schiff base ligand MCPMP-EA was carried out. X-ray intensity data were collected on Bruker CCD area-detector diffractometer equipped with graphite monochromated MoKα radiation (λ=0.71073 Å) at 23 °C. The crystal used for data collection was of dimensions 0.30×0.20×0.20 mm. The cell dimensions were determined by least-square fit of angular settings of 5610 reflections in the θ range $2.48<\theta<25.00^o$. The intensities were measured by Ø and ω scan mode for θ range 3.42 to25.00^o.2965reflectionsweretreatedasobserved(I>2σ(I)).DatawerecorrectedforLorentz, polarization and absorption factors. The structure was solved by direct methods using SHELXS97 [152]. Allnon-hydrogenatomsofthemoleculewerelocatedinthebest E-map.Full-matrixleast-squaresrefinementwascarriedoutusingSHELXL97[152]. AtomicscatteringfactorsweretakenfromInternationalTablesforX-rayCrystallography(1992,Vol.C,Tables4.2.6.8and6.1.1.4).AnORTEP[153]viewof theligandwithatomic labelingisshowninFigure

[304].Thegeometryofthemoleculehasbeencalculatedusingthe softwarePLATON[154] and PARST [155].

3.2.3DNA BindingExperiments

Absorption titration experiments forboth the complexes were performed by maintainingconstantmetalcomplexconcentrationof1mMwhilevaryingtheconcentration of CT-DNAwithin0μMto350μM. Fromtheabsorptiondata, theintrinsicbindingconstantK_b wasdeterminedfromaplotof[DNA]/($\varepsilon_a-\varepsilon_f$) versus[DNA] usingthe equation:

$$[DNA]/(\varepsilon_a-\varepsilon_f)=[DNA]/(\varepsilon_b-\varepsilon_f)+[K_b(\varepsilon_b-\varepsilon_f)]^{-1}$$

where, [DNA] is the concentration of DNA in base pairs. The apparentabsorptioncoefficientsε_a,ε_f,andε_b correspondtoA_{obsd}/[M](whereM=metal=Cu^{+2}),totheextinction coefficientforthefreeCu(II)complexandtotheextinctioncoefficient for the Cu(II)complexin thefullybound form, respectively.

FluorescencequenchingexperimentswereconductedbyaddingCu(II)complex solution at different concentrations tothesamplescontaining3.3μMEBand3μM DNA in buffer (150 mM NaCl and 15 mM trisodium citrate at pH 7.03). Allthe samples wereexcited at546 nm and emission was recordedat 550–750 nm. The Stern–Vormer constant K_{sv} for each complex was calculated according to the following Eq.:

$$F_0/F = 1 + K_{sv}[Q]$$

Where, F_0 and F are the emission intensities in the absence and presence of quencher respectively, Q is the concentration of the quencher and K_{sv} is the Stern–Vormer constant, obtained from the slope of the plot of F_0/F versus [Q].

Viscosity experiments were carried out by using an Ostwald's capillary viscometer, immersed in a thermostated water bath with the temperature setting at 30 ± 0.1 °C for 15 min. DNA samples with an approximate average length of 200-500 base pairs were prepared by sonication in order to minimize complexities arising from DNA flexibility [267]. Flow time was measured with a digital stopwatch. Each sample was measured in triplicate and an average flow time was considered for final calculation. Data were presented as $(\eta/\eta_0)^{1/3}$ versus the mole ratio of Cu(II) complex to DNA. Where η is the viscosity of DNA in the presence of complex, and η_0 is the viscosity of DNA alone.

3.3 Preparation of Schiff base ligands and metal complexes

3.3.1Synthesis of 4-((E)-(2-hydroxyethylimino)(p-tolyl)methyl)-3-methyl-1-phenyl-1H-pyrazol-5-ol [PMP-EA]

PMP (2.92 gm, 10 mmol) was dissolved in minimum amount of absolute ethanol. To this solution, a solution of 2-ethanolamine (0.7 ml, 10 mmol) in 20 ml ethanol was added drop wise. The reaction mixture was refluxed for 6 hours. After cooling, a microcrystalline yellow compound was separated. The Schiff baseligand was filtered and washed with water and then with ethanol and dried under vacuum. (Scheme-3.1)

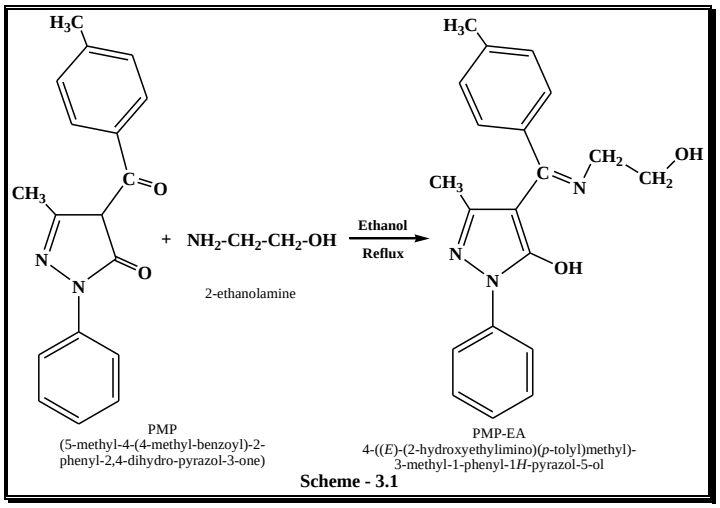

Scheme - 3.1

PMP-EA is yellow crystalline compound. Yield: 81.85%, m.p.: 150^{o}C. Anal. Calc. for $C_{20}H_{21}N_3O_2$ M.W.: 335.40, C(71.62%), H(6.31%), N(12.53%), found: C(71.28%), H(6.21%), N(12.91%).

IR (KBr, cm^{-1}): 3354(m) (O–H), 2924(m) (N-H), 1536(s) (C=N, cyclic), 1615(m) (C=O, pyrazolone ring), 1222(s) (C=N, azomethane).^{1}H NMR ($CDCl_3$, 400 MHz, TMS): δ1.80(s,3H,PZC-CH_3),3.19 (s, 3H,TLC−CH_3),7.02-7.41(m,5H,Ph), 7.99-8.07(m, 4H,TL),5.07(m, 1H,-OH), 3.42-3.45(t,2H, N-CH_2-), 3.37-3.40(t,3H,-CH_2-O), 11.23(s, 1H,-NH).MASS: m/z = 257.14 $[C_{14}H_{16}N_3O_2]^+$, 97.08 $[C_4H_4N_2O]^+$.

3.3.2Synthesis of 4-((E)-(2-hydroxyethylimino)(p-tolyl)methyl)-1-(3-chlorophenyl)-3-methyl-1H-pyrazol-5-ol [MCPMP-EA]

MCPMP (3.26 gm, 10 mmol) was dissolved in minimum amount of absolute ethanol. To this solution, a solution of 2-ethanolamine (0.7 ml,10 mmol) in 20 ml ethanol was added drop wise. The reaction mixture was refluxed for 6 hours. After cooling, a microcrystalline yellow compound was separated. The Schiff baseligand was filtered and washed with water and then with ethanol and dried under vacuum. (Scheme-3.2)

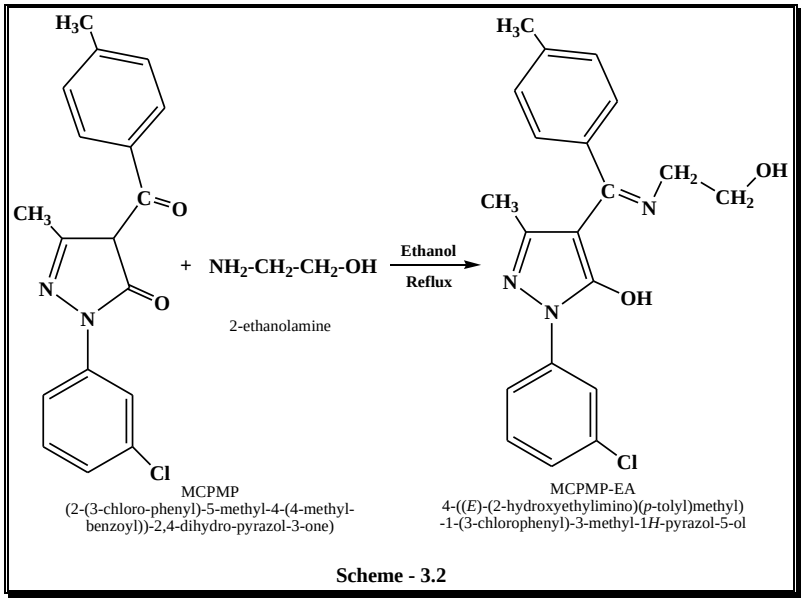

MCPMP
(2-(3-chloro-phenyl)-5-methyl-4-(4-methyl-benzoyl))-2,4-dihydro-pyrazol-3-one)

MCPMP-EA
4-((*E*)-(2-hydroxyethylimino)(*p*-tolyl)methyl)-1-(3-chlorophenyl)-3-methyl-1*H*-pyrazol-5-ol

Scheme - 3.2

MCPMP-EA is yellow crystalline compound. Yield: 82.68%, m.p.: 165^{o}C. Anal. Calc. for $C_{20}H_{20}ClN_3O_2$ M.W.: 369.84, C(64.95%), H(5.45%), N(9.59%), found: C(64.41%), H(5.29%), N(9.66%).

IR (KBr, cm^{-1}): 3418(m) (O–H), 2923(m) (N-H), 1539(s) (C=N, cyclic), 1620(m) (C=O, pyrazolone ring), 1227(s) (C=N, azomethane).^{1}H NMR ($CDCl_3$, 400 MHz, TMS): δ1.39(s,3H,PZC-CH_3),3.20 (s, 3H,TLC-CH_3),7.09-7.60(m,4H,Ph), 7.96-8.05(m, 4H,TL),5.08(s, 1H,-OH), 3.41-3.46(t,2H, N-CH_2-), 3.49-3.52(t,2H,-CH_2-O), 11.26(s, 1H, -NH). MASS: m/z = 369.10 $[C_{20}H_{20}ClN_3O_2]^+$, 339.14 $[C_{18}H_{14}ClN_3O_2]^+$, 264.17 $[C_{12}H_{10}ClN_3O_2]^+$, 257.15 $[C_{14}H_{16}N_3O_2]^+$, 97.07 $[C_4H_4N_2O]^+$.

3.3.3Synthesis of 4-((E)-(2-hydroxyethylimino)(p-tolyl)methyl)-3-methyl-1-p-tolyl-1H-pyrazol-5-ol [PTPMP-EA]

PTPMP (3.0 gm, 10 mmol) was dissolved in minimum amount of absolute ethanol. To this solution, a solution of 2-ethanolamine (0.7 ml, 10 mmol) in 20 ml ethanol was added drop wise. The reaction mixture was refluxed for 6 hours. After cooling, a microcrystalline yellow compound was separated. The Schiff base ligand was filtered and washed with water and then with ethanol and dried under vacuum. (Scheme-3.3)

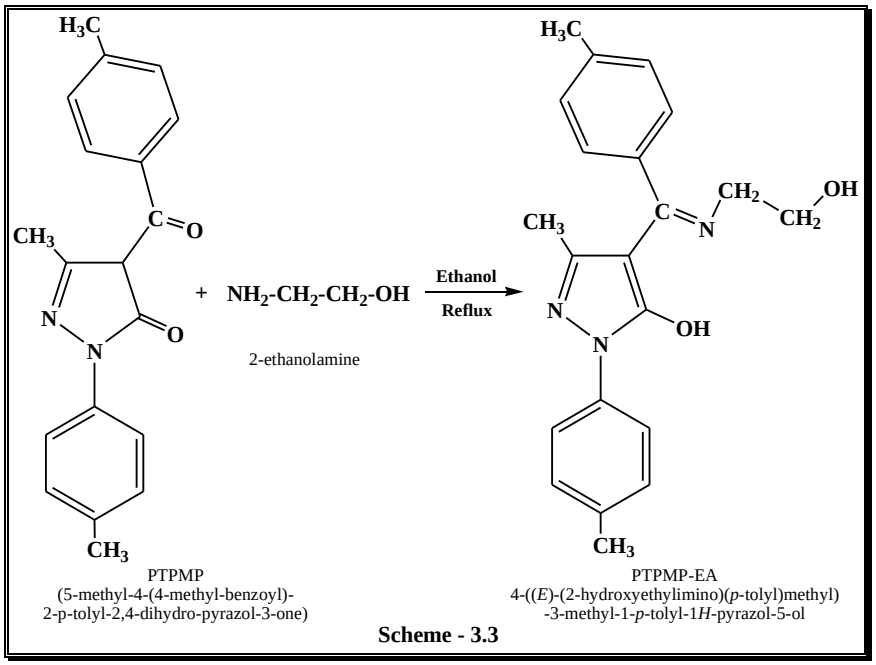

PTPMP
(5-methyl-4-(4-methyl-benzoyl)-
2-p-tolyl-2,4-dihydro-pyrazol-3-one)

PTPMP-EA
4-((*E*)-(2-hydroxyethylimino)(*p*-tolyl)methyl)
-3-methyl-1-*p*-tolyl-1*H*-pyrazol-5-ol

Scheme - 3.3

PTPMP-EA is light yellow crystalline compound. Yield: 80.85%, m.p.: 160^{o}C. Anal. Calc. for $C_{21}H_{23}N_3O_2$ M.W.: 349.43, C(72.18%), H(6.63%), N(12.03%), found: C(72.68%), H(6.21%), N(12.51%).

IR (KBr, cm^{-1}): 3347(m) (O–H), 2923(m) (N-H), 1526(s) (C=N, cyclic), 1607(m) (C=O, pyrazolone ring), 1220(s) (C=N, azomethane).δ1.34(s,3H,PZC-CH_3),3.18 (s, 3H,TLC-CH_3),7.07-7.39(m,5H,Ph), 7.86-7.94(m, 4H,TL),5.05(s, 1H,-OH), 3.44-3.45(t,2H, N-CH_2-), 3.49-3.50(t,2H,-CH_2-O), 11.24(s, 1H, -NH).MASS: m/z = 349.28 $[C_{21}H_{23}N_3O_2]^+$, 348.10 $[C_{21}H_{22}N_3O_2]^+$, 200.03 $[C_{11}H_9N_2O_2]^+$, 119.13 $[C_8H_7O]^+$, 90.06 $[C_7H_7]^+$.

3.3.4 Synthesis of [Cu(PMP-EA)(H_2O)$_2$]

Cu-acetate (2 mmol) was dissolved in minimum amount of water and the solution was added to a hot ethanolic solution of PMP-EA (0.66gm, 2 mmol). A

crystalline solid was formed which was filtered, washed with hot distilled water and then from ethanol and dried under vacuum. (Scheme – 3.4)

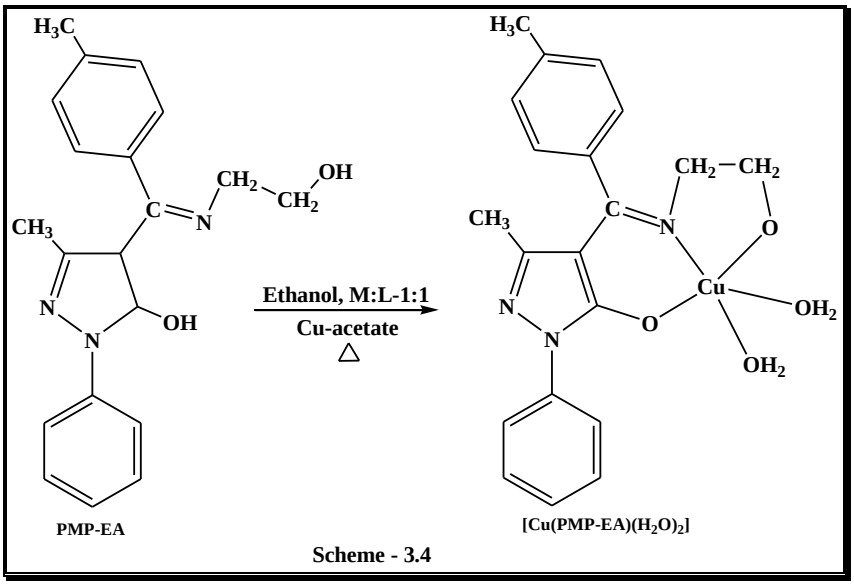

Scheme - 3.4

$[Cu(PMP\text{-}EA)(H_2O)_2]$ is green crystalline compound. Yield: 58.62%, m.p.: 250^oC, Solubility: DMF. Anal. Calc. for $C_{20}H_{23}CuN_3O_4$ M.W.: 432.96, C(55.48%), H(5.35%), N(9.71%), Cu(14.68%),found: C(55.95%), H(5.76%), N(9.72%), Cu(14.81%).

IR (KBr, cm^{-1}):3429(m) (O-H coordinated H_2O), 1579(s) (C=N, cyclic), 1494(m) (C-O), 449 (m) (Cu-N), 474(m) (Cu-O);MS: *m/z* = 431.2 $[C_{20}H_{22}CuN_3O_4]^+$, 370.3 $[C_{18}H_{17}CuN_3O_2]^+$, 372.3 $[C_{18}H_{19}CuN_3O_2]^+$, 327.2 $[C_{12}H_{15}CuN_3O_4]^+$, 235.1 $[C_7H_{14}CuN_3O_2]^+$, 202.3 $[C_{11}H_{11}N_3O]^+$, 122.0 $[C_5H_7N_3O]^+$

3.3.5 Synthesis of [Cu(MCPMP-EA)(H₂O)₂]

Cu-acetate (2 mmol) was dissolved in minimum amount of water and the solution was added to a hot ethanolic solution of MCPMP-EA (0.93gm, 2 mmol). A crystalline solid was formed which was filtered, washed with hot distilled water and then from ethanol and dried under vacuum. (Scheme – 3.5)

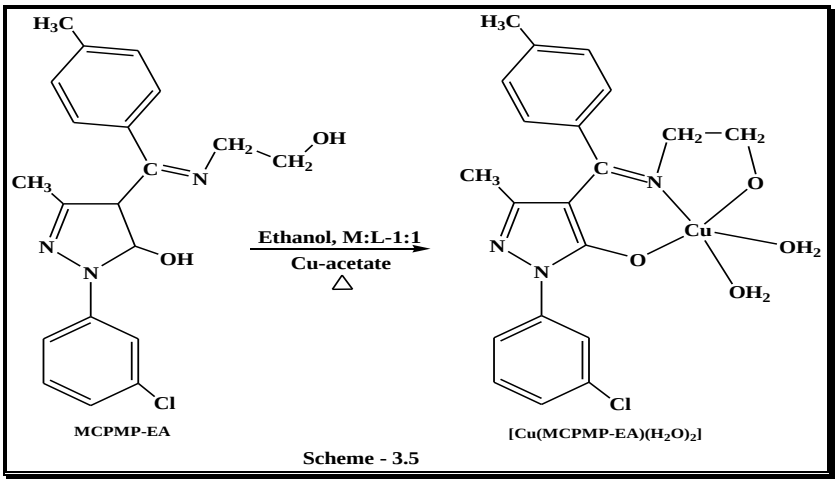

Scheme - 3.5

$[Cu(MCPMP\text{-}EA)(H_2O)_2]$ is dark green crystalline compound. Yield: 59.86%, m.p.: 260^{o}C, Solubility: DMF. Anal. Calc. for $C_{20}H_{22}ClCuN_3O_4$ M.W.: 467.41, C(51.39%), H(4.74%), N(8.99%), Cu(13.60%), found: C(51.68%), H(4.67%), N(8.54%), Cu(13.51%).

IR (KBr, cm^{-1}):3430(m) (O-H coordinated H_2O), 1596(s) (C=N, cyclic), 1480(m) (C-O), 445 (m) (Cu-N), 468(m) (Cu-O);MS: *m/z* = 470.4 [M+2 peak, $[C_{20}H_{22}ClCuN_3O_4]^+$, 431 $[C_{20}H_{18}ClCuN_3O_2]^+$, 398.3 $[C_{20}H_{19}CuN_3O_2]^+$, 307.3 $[C_{13}H_{13}CuN_3O_2]^+$, 381.2 $[C_{19}H_{17}CuN_3O_2]^+$, 350.3 [Basepeak, $C_{18}H_{13}CuN_3O]^+$, 351.3 $[C_{18}H_{14}CuN_3O]^+$, 307.3 $[C_{18}H_{17}N_3O_2]^+$.

3.3.6 Synthesis of [Cu(PTPMP-EA)(H$_2$O)$_2$]

Cu-acetate (2 mmol) was dissolved in minimum amount of water and the solution was added to a hot ethanolic solution of PTPMP-EA (0.89gm, 2 mmol). A crystalline solid was formed which was filtered, washed with hot distilled water and then from ethanol and dried under vacuum. (Scheme – 3.6)

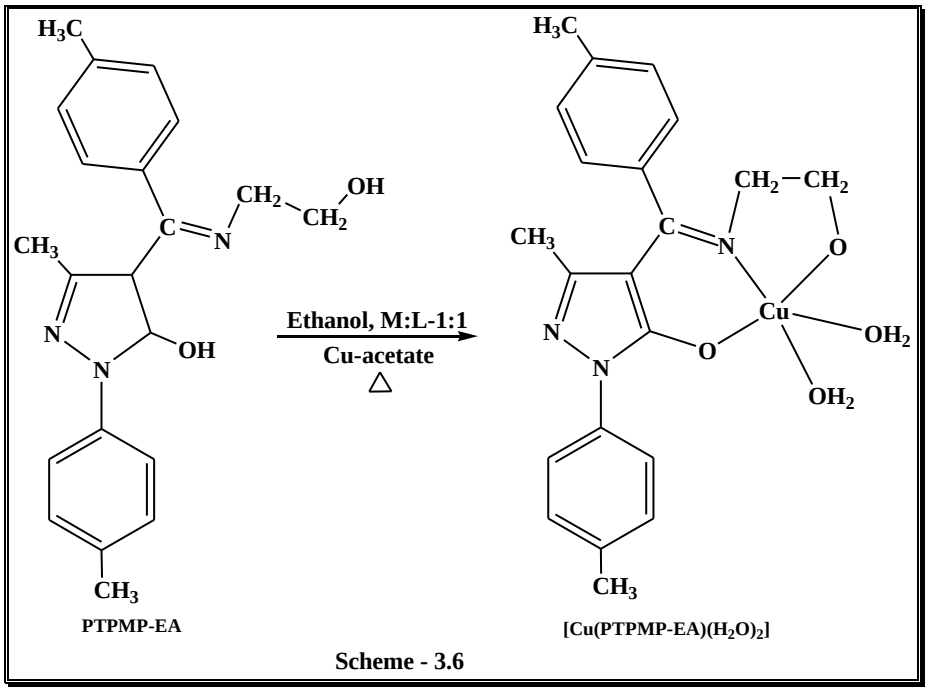

Scheme - 3.6

[Cu(PTPMP-EA)(H_2O)$_2$] is green crystalline compound. Yield: 55.76%, m.p.: 250^{o}C, Solubility: DMF. Anal. Calc. for $C_{21}H_{25}CuN_3O_4$ M.W.: 446.99, C(56.43%), H(5.64%), N(9.40%), Cu(14.22%), found: CC(56.75%), H(5.96%), N(9.72%), Cu(14.61%).

IR (KBr, cm^{-1}):3436(m) (O-H coordinated H_2O), 1597(s) (C=N, cyclic), 1477(m) (C-O), 430 (m) (Cu-N), 478(m) (Cu-O);MS: *m/z* = 446.11 $[C_{21}H_{25}CuN_3O_4]^+$, 410.9 $[C_{21}H_{21}CuN_3O_2]^+$, 396 $[C_{20}H_{19}CuN_3O_2]^+$, 368 $[C_{18}H_{15}CuN_3O_2]^+$, 292 $[C_{12}H_{11}CuN_3O_2]^+$, 216 $[C_6H_7CuN_3O_2]^+$, 155 $[C_6H_9N_3O_2]^+$.

3.4Characterization of Schiff base ligands and metal complexes

3.4.1 Physico-chemical properties of synthesized Schiff base ligands and metal complexes

Theligandswerepreparedbyrefluxinganappropriateamountofrespective4-toluoyl pyrazolonewith2-ethanolamineinethanol.Thestructuresofthesynthesizedligandswere establishedwiththehelpoftheirIR,NMRandmicro analyticaldataandthedataconcurredwell withthe plannedformulaeofligands. Cu(II) complexesof these ligands were preparedbyusingcopper acetatewiththecorrespondingligand in1:1 molar ratio.Allthesecomplexesareintensively green colored,airandmoisturefreeamorphoussolids.

Theyareinsolubleincommonorganicsolventsandonlysolubleinin DMFandDMSO.Molar conductancevaluesofthecomplexes solubleinDMF(10^{-3}M solutionat25°C)indicatethatthe complexes havemolarratioofmetal: ligandas1:1.

3.4.2 Crystal structure of Schiff base ligand

3.4.2.1. *The Crystal structure of Schiff base ligandMCPMP-EA*

X-raystructuredeterminationrevealsthattheketotautomerismfavoredovertheenol-formfortheSchiffbase.Thisisevidentfromtheobserved bonddistances.C=Obonddistanceof1.259A°,whichisconsistentwiththeC=Odoublebond indicatingmorecharacteristicofketonethanC-OHbond.Thehighconfigurationeffectexistinginthepyrazolone-ringinducesanarrowrangeofbonddistances. Similarly,theC13–N21distanceof1.316A°isalsoagreementwithaC=Ndouble bond andC5–N1withadistanceof1.381A° isapparently a singlebond.In thecompound, there areintermolecularhydrogenbonds,buttherewasnointramolecularhydrogenbondinthecrystal. (Figure 3.1 & Table 3.1, 3.2)

Figure- 3.1: ORTEP view of Schiff base ligand MCPMP-EA

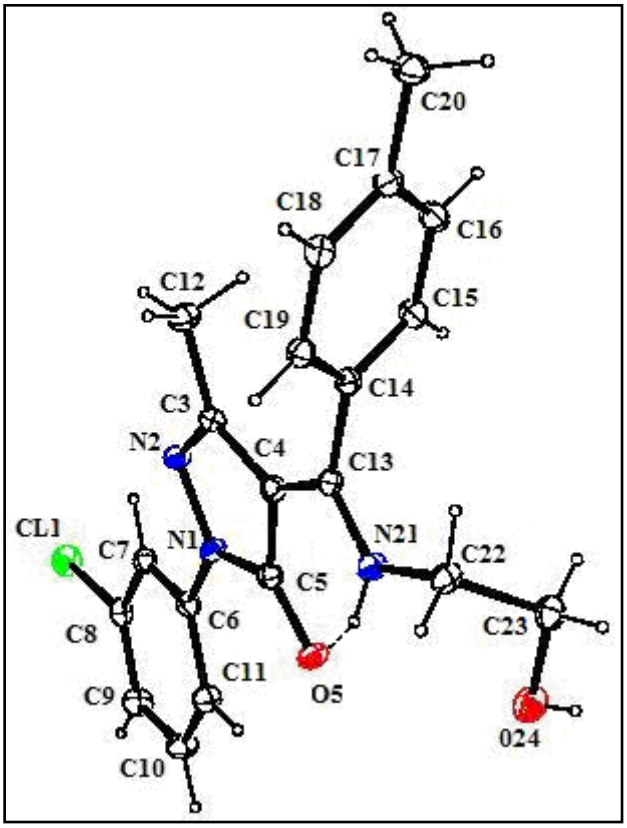

***ORTEP* view of the molecule with displacement ellipsoids drawn at 50% probability level. H atoms are shown as small spheres of arbitrary radii.**

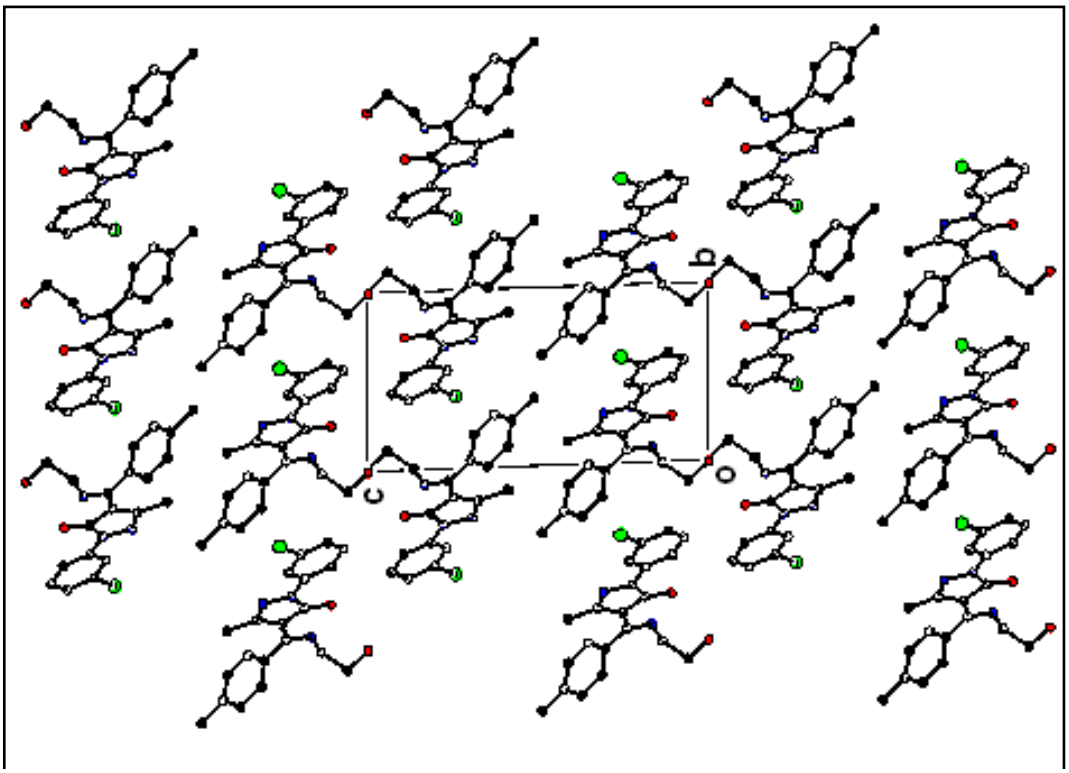

The packing arrangement of molecules viewed down the a-axis.

Table-3.1: Crystallographic data of Schiff base ligand MCPMP

Compound	MCPMP-EA
Chemical formula	C_{20} H_{20} Cl N_3 O_2
Formula weight	369.84
Crystal description	White plate
a(Å)	7.0934(15)
b(Å)	8.9452(19)
c(Å)	15.861(3)
α(°)	89.387(4)
β(°)	83.801(4)
γ (°)	66.970(4)
Z	2
V(Å^3)	920.3(3)
Reflection collected/unique	4692/ 3162
R(int)	0.0265
Number of parameters	240
Crystal system, Space group	Triclinic, P-1
Limiting indices	h= -8 to7 , k= -10 to 9, l= -15 to 18
Crystal size	0.3 x 0.2 x 0.2 mm
$\rho_{calcd.}$(g cm^{-3})	1.335
Abs coeff, μ(cm^{-1})	0.227
F(000)	388
Temp(°C)	23
GOF on F^2	1.003

Table3.2: Selected bond lengths and bond angles of MCPMP

Bond distances (Å) with esd in parentheses		Bond angles(°) with esd in parentheses	
O5 C5	1.259(2)	C5 N1 C6	128.96(18)
N21 C22	1.453(3)	O5 C5 N1	126.24(19)
C23 O24	1.422(3)	C7 C8 Cl1	118.48(17)
Cl1 C8	1.743(2)	C7 C6 N1	118.73(18)
N1 C5	1.381(3)	C11 C6 N1	121.25(19)
N1 C6	1.412(3)	N2 C3 C12	118.73(18)
N2 C3	1.306(3)	N2 C3 C4	112.02(18)

3.4.3 IR spectral studies

The bonding mode of the ligand coordinated to Cu(II) ion was further elucidated by comparison of the IR spectra of the ligands and Cu-complexes. From the crystal structure, we can see that the ligand exists as the keto form in solid state. The broad peak at ~2923 cm^{-1} in the free ligands corresponds to the *ν*(N–H). And the strong bands at ~1536 and ~1615 cm^{-1} are assigned to *ν*(C=N) and *ν*(C=O) of the pyrazolones ring, which bears out that ligand exists as the keto form in the solid state, consistent with the crystal structure.

In IR spectra of the complexes, it is clearly observed that the C=O and N–H

stretching vibrations disappear, and new band attributed to *v*(C–O) appears at ~1480 cm^{-1}. There are other changes that the absorption peaks of C–OH and C=N slightly shift to lower wave number, indicating the coordination of oxygen from 2-hydroxyethylimino group and azomethane nitrogen to the central metal atom. In addition, the new bands at about 445 and 468 cm^{-1} are assigned to Cu–N and Cu–O stretching vibrations. These results indicate that the ligand undergoes isomerization from the keto form to the enol form during the coordination, and then loses two protons to coordinate with Cu(II) atom as a double negative charged bidentate ligand [268,269]. Furthermore, the lateral chain of the ligand occur torsion nearly 180° going with losing protons. This perhaps resulted by the coordination effect of the copper ion. (Figure 3.2-3.6)

Figure 3.2: IR spectrum of Schiff base ligand PMP-EA

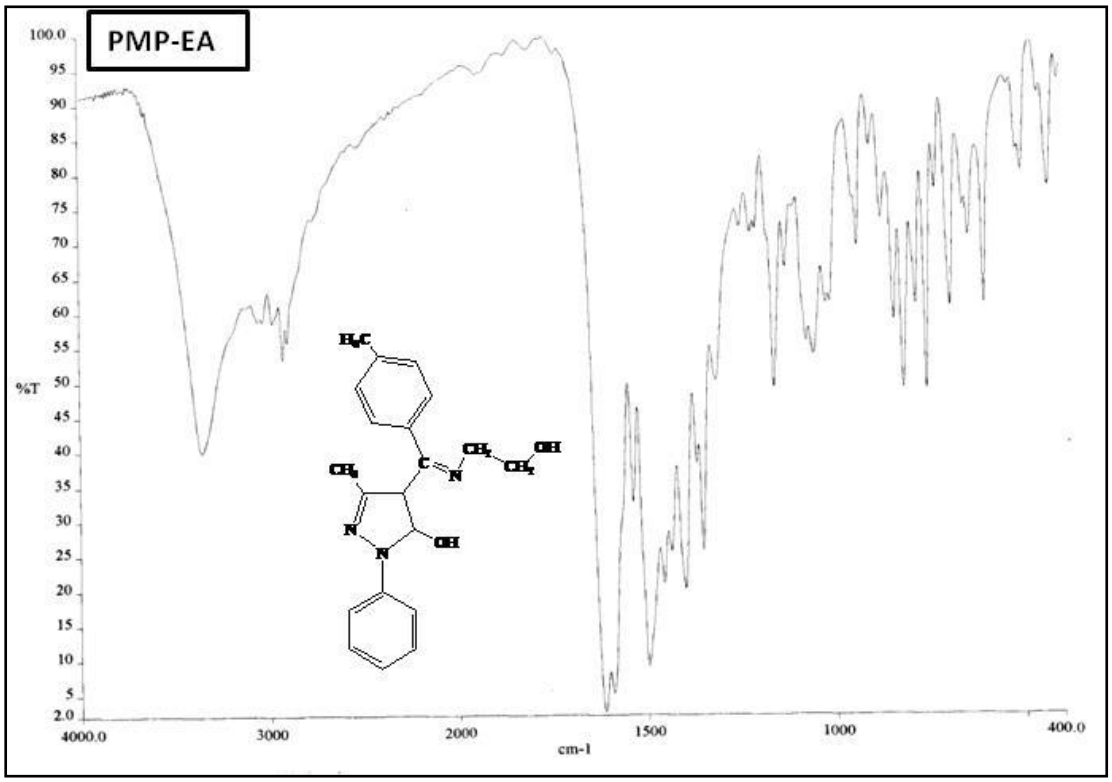

Figure 3.3: IR spectrum of Schiff base ligand MCPMP-EA

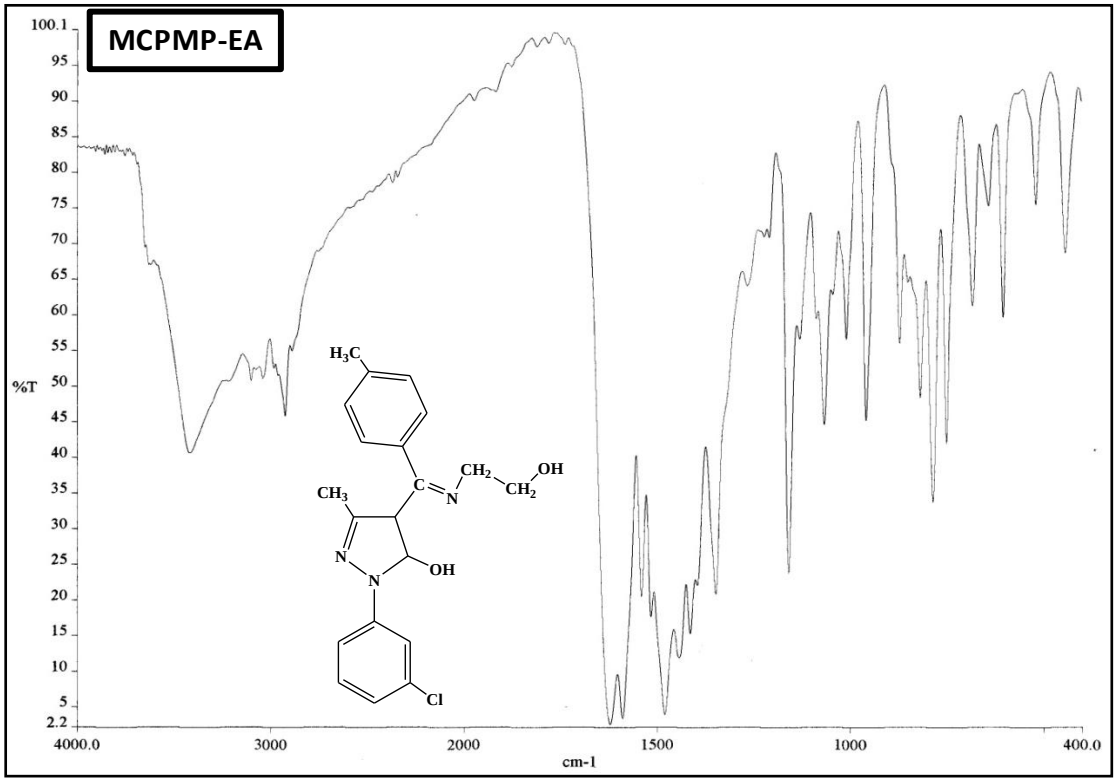

Figure 3.4: IR spectrum of Schiff base ligand MCPMP-EA

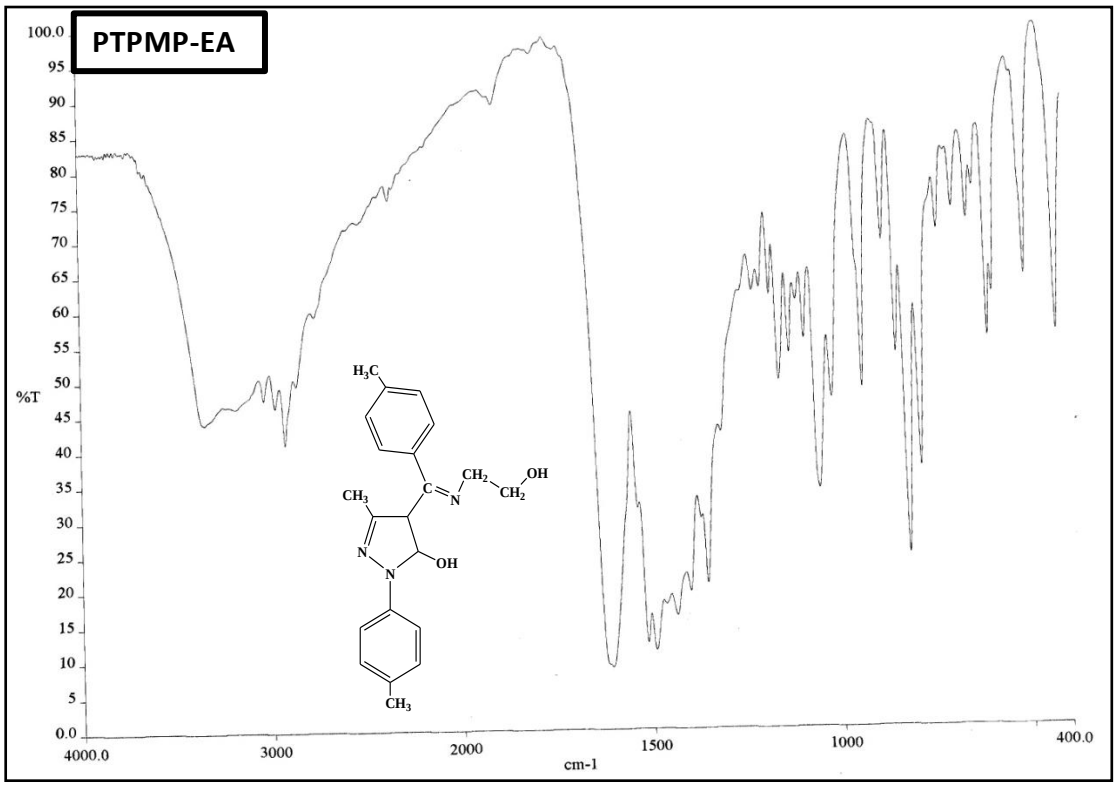

Figure 3.5: IR spectrum of metal complex [Cu(MCPMP-EA)(H_2O)$_2$]

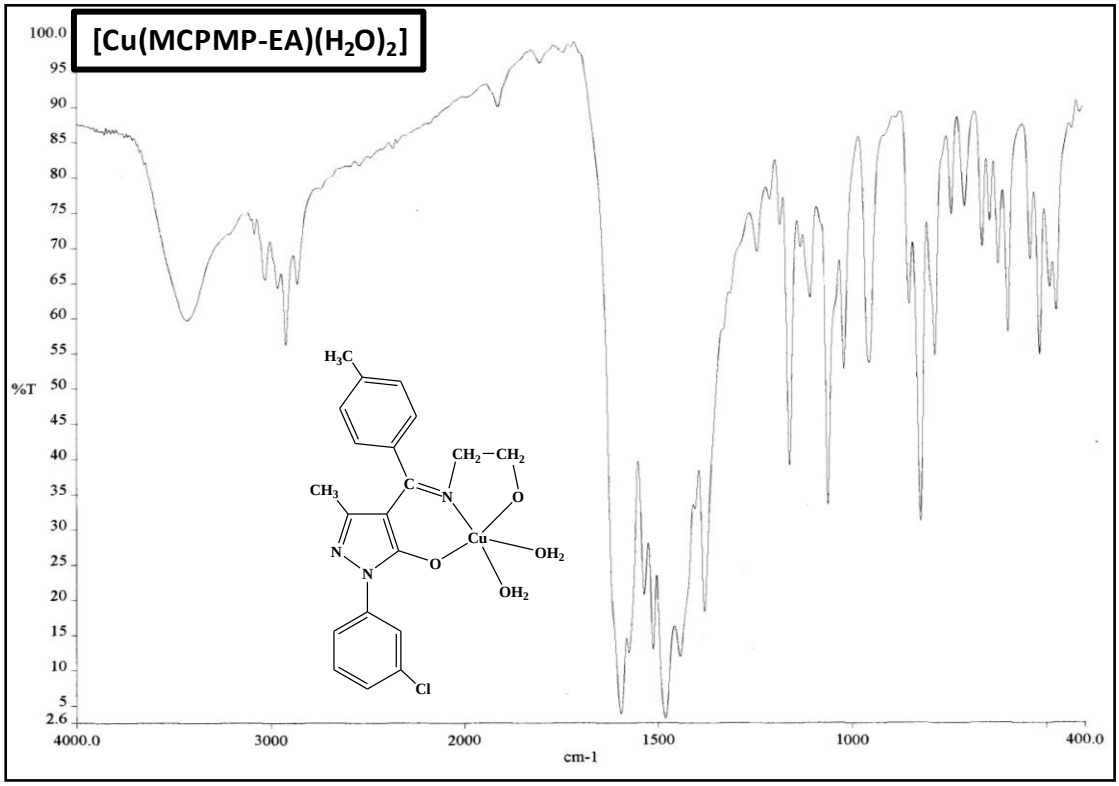

Figure 3.6: IR spectrum of metal complex [Cu(PTPMP-EA)(H_2O)$_2$]

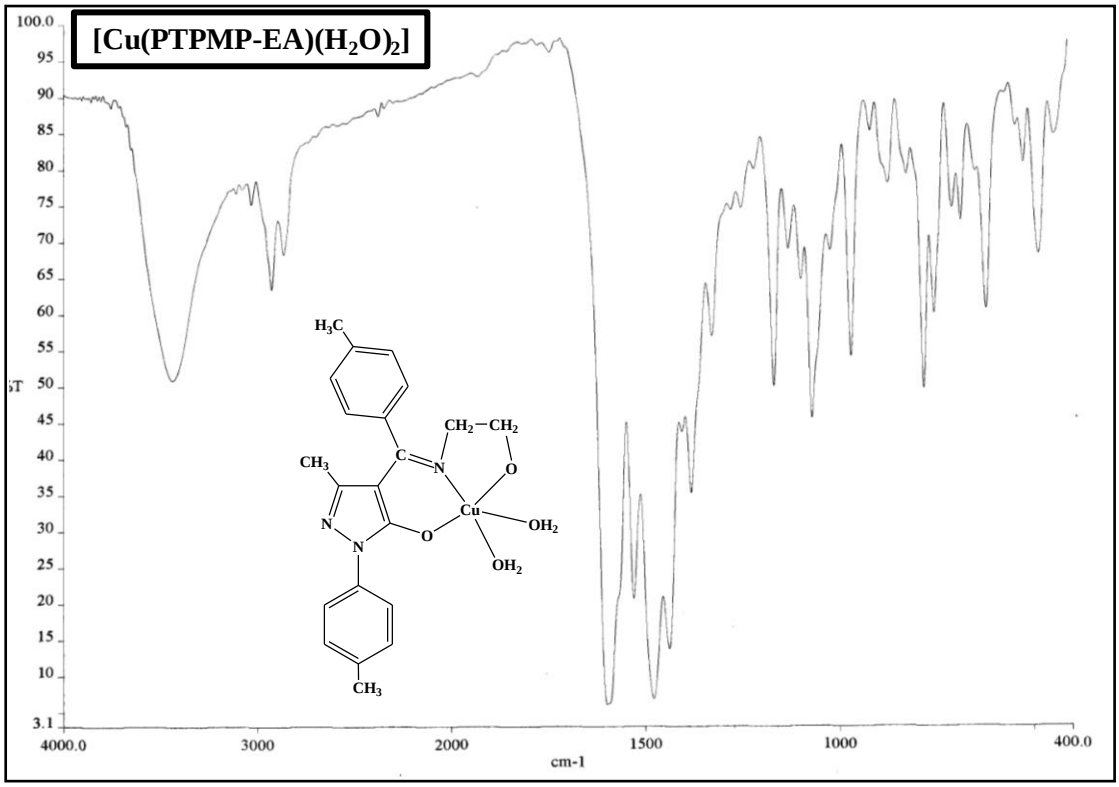

3.4.4 NMR spectral studies

The ^{1}Hspectraof theligandswerecarriedoutinDMSO-d^{6} atroomtemperature. Thedataarereportedalongwiththepossibleassignmentsin"experimental" section.Alltheprotonswere found as tobein their expected region [270,271]. (Figure 3.7-3.11)

Figure 3.7: ^{1}H NMR spectrum of Schiff base ligand PMP-EA

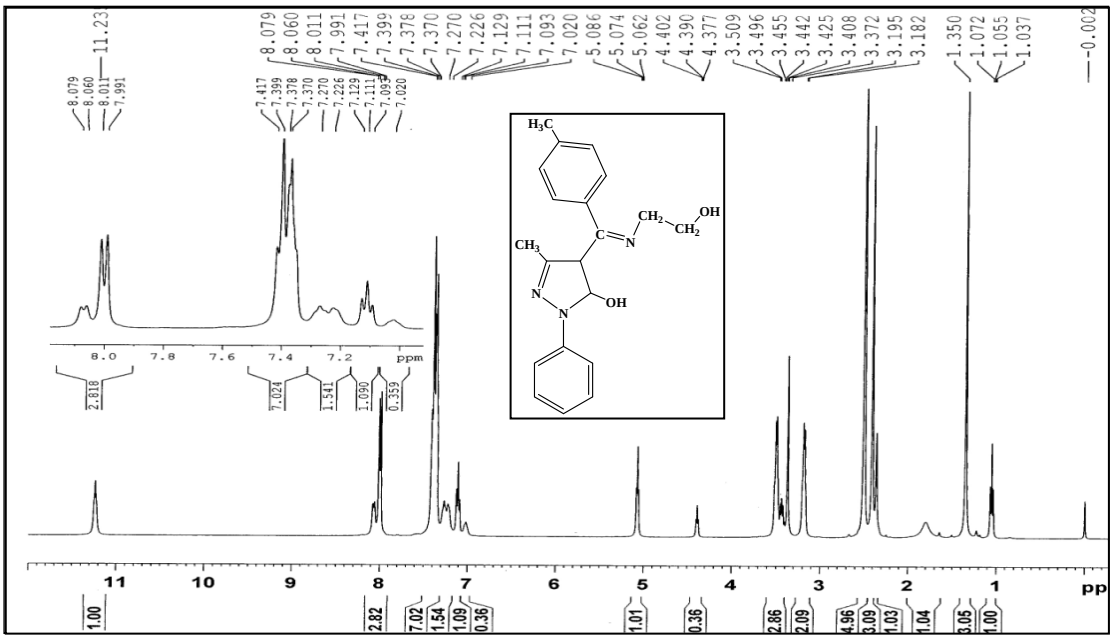

Figure 3.8: ^{1}H NMR spectrum of Schiff base ligand MCPMP-EA

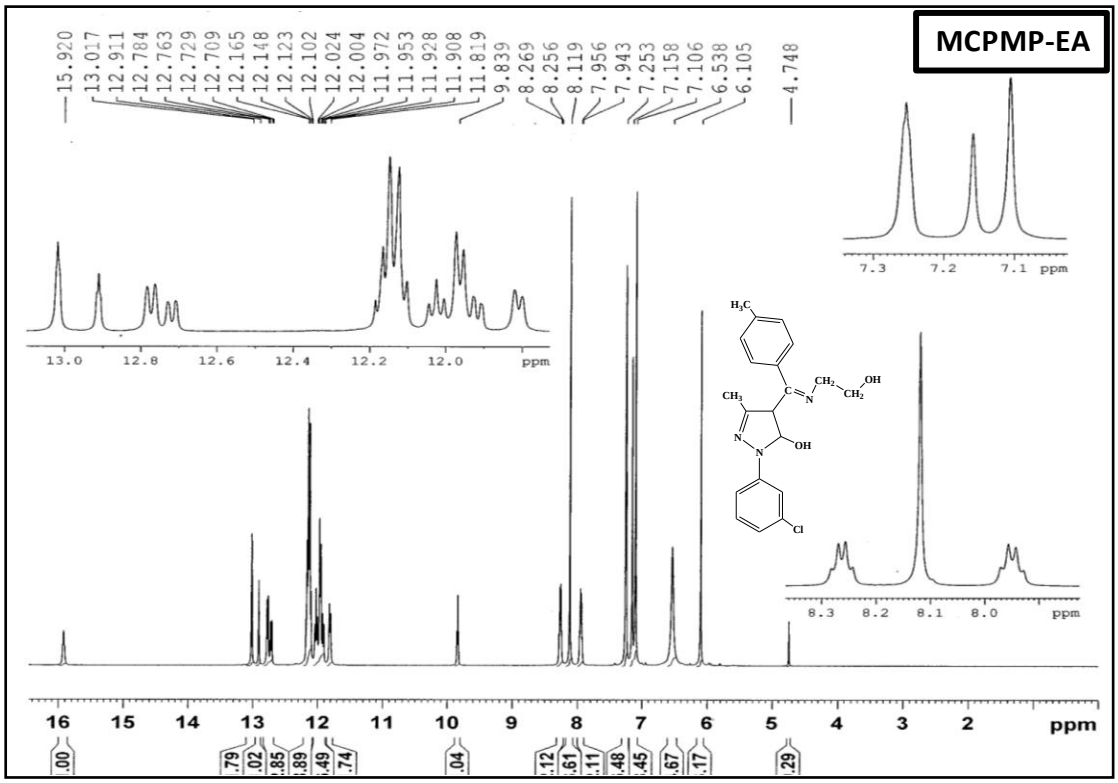

Figure 3.9: ^{13}C NMR spectrum of Schiff base ligand PMP-EA

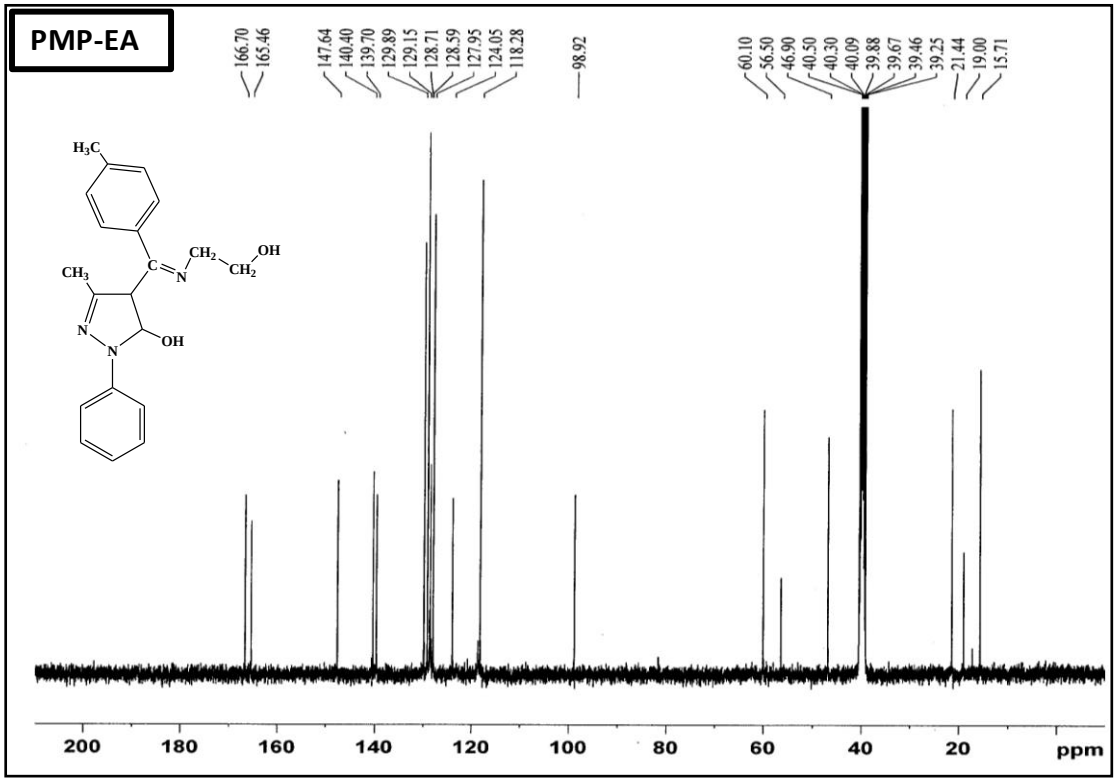

Figure 3.10: ^{13}C NMR spectrum of Schiff base ligand MCPMP-EA

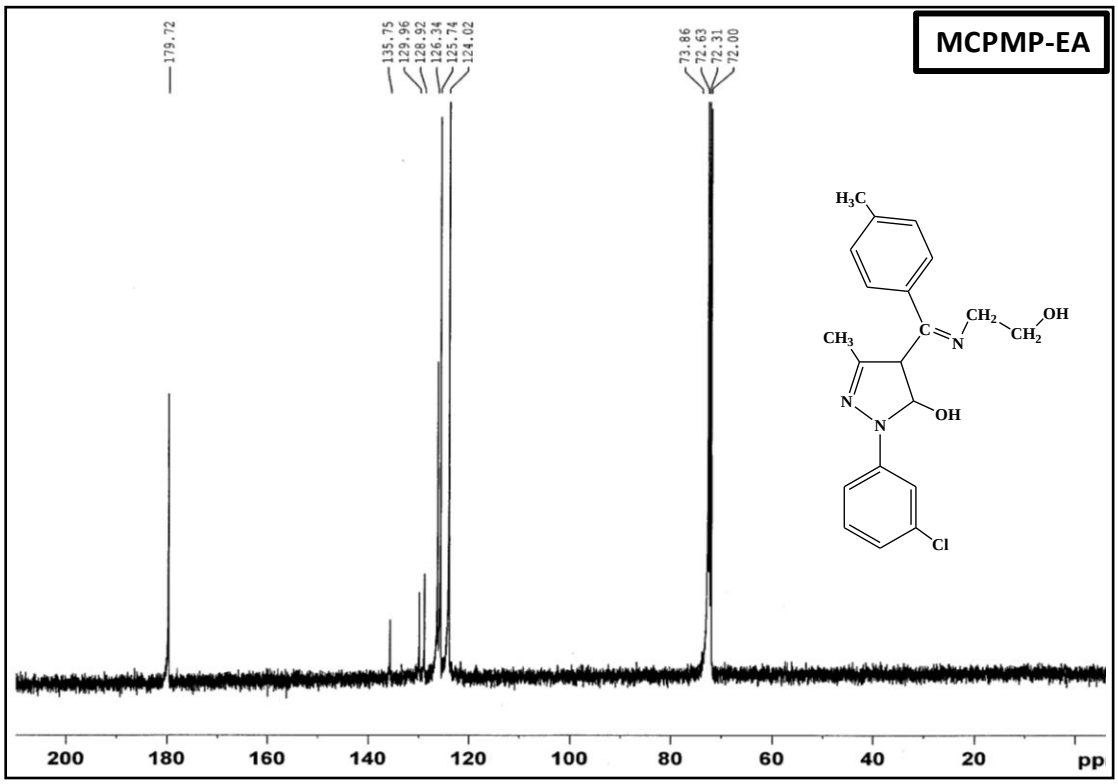

Figure 3.11: ^{13}C NMR spectrum of Schiff base ligand PTPMP-EA

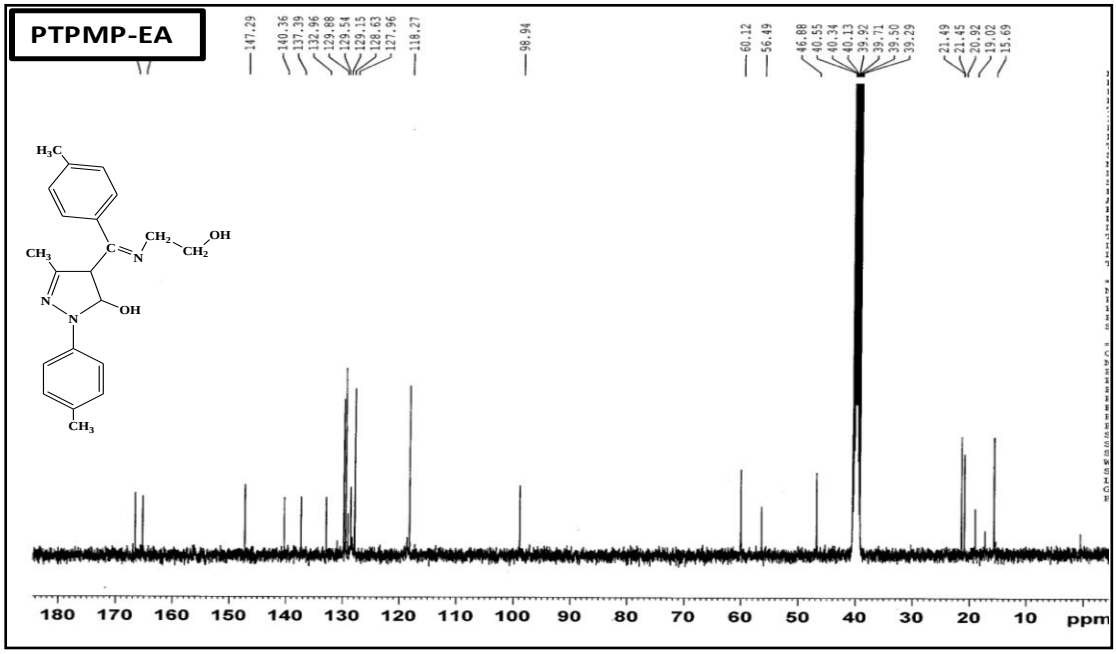

3.4.5 Mass spectral studies

Theelectronimpactmassspectraldataofschiffbases and complexesarereportedin"experimental" section.All thecomplexesgiveamolecularionpeakcorresponding to their molecular weight.Theintensitiesofthesepeaksgivetheideaofthestabilityandabundanceofthe fragments.Thistypeofstoichiometry[$ML(H_2O)_2$]isconfirmedbythemassspectraofother complexes.Thisisingoodagreementwiththe micro analytical data. [202,270,272](Figure 3.12-3.15)

Figure 3.12: Mass spectrum of Schiff base ligand PMP-EA

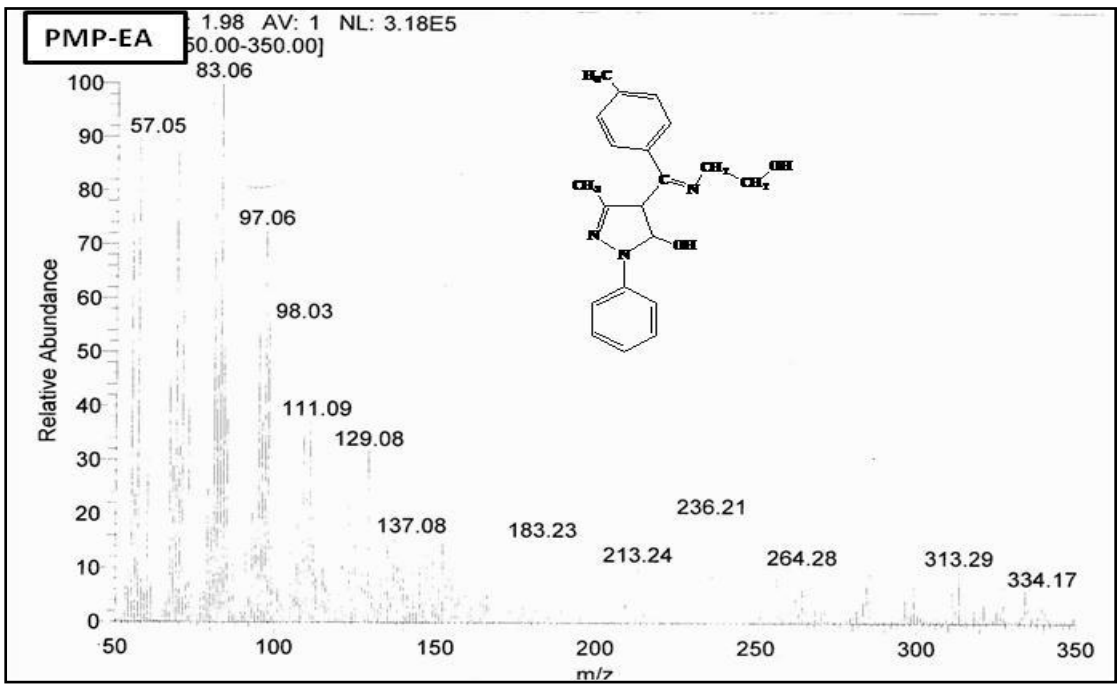

Figure 3.13: Mass spectrum of Schiff base ligand MCPMP-EA

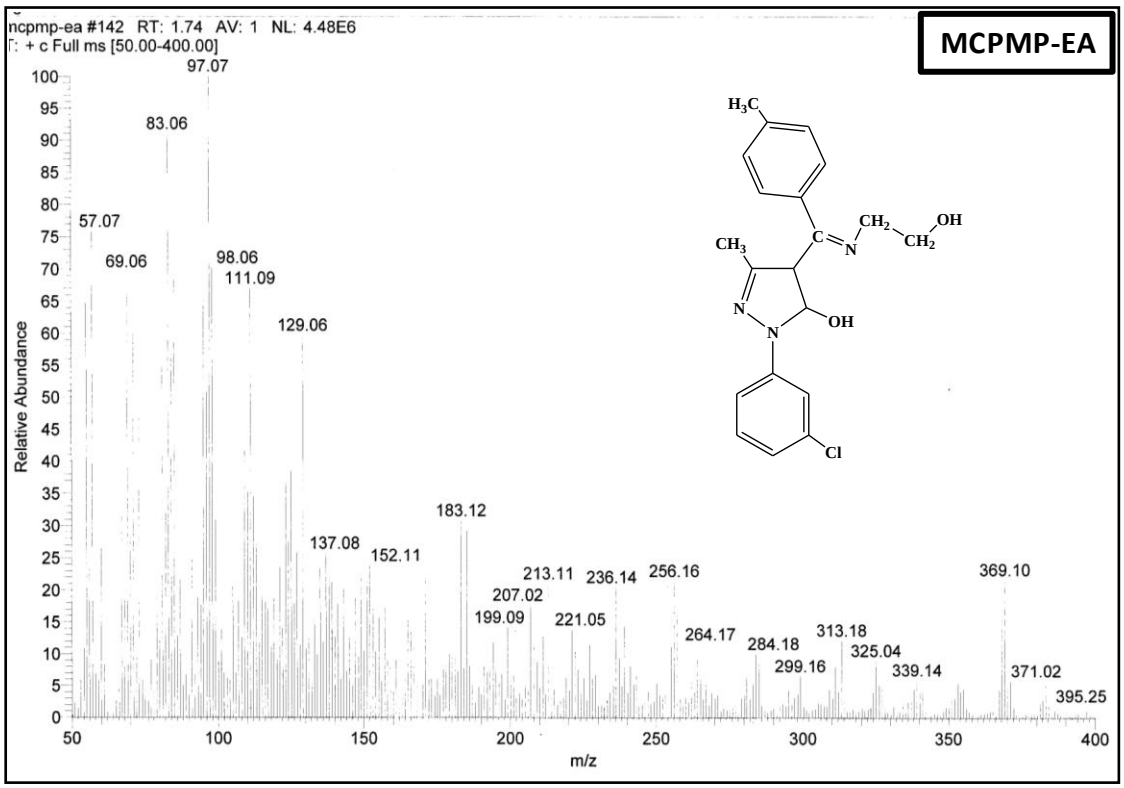

Figure 3.14: Mass spectrum of Schiff base ligand PTPMP-EA

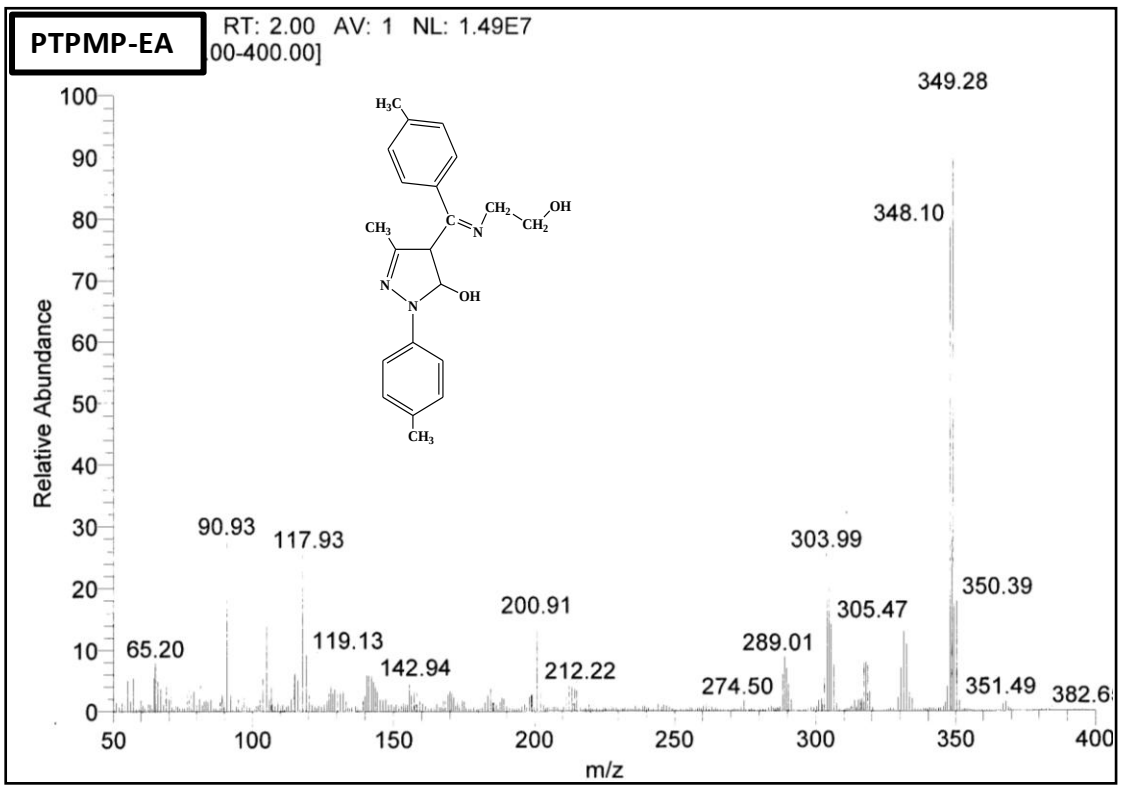

Figure 3.15: Mass spectrum of metal complex [Cu(MCPMP-EA)(H_2O)$_2$]

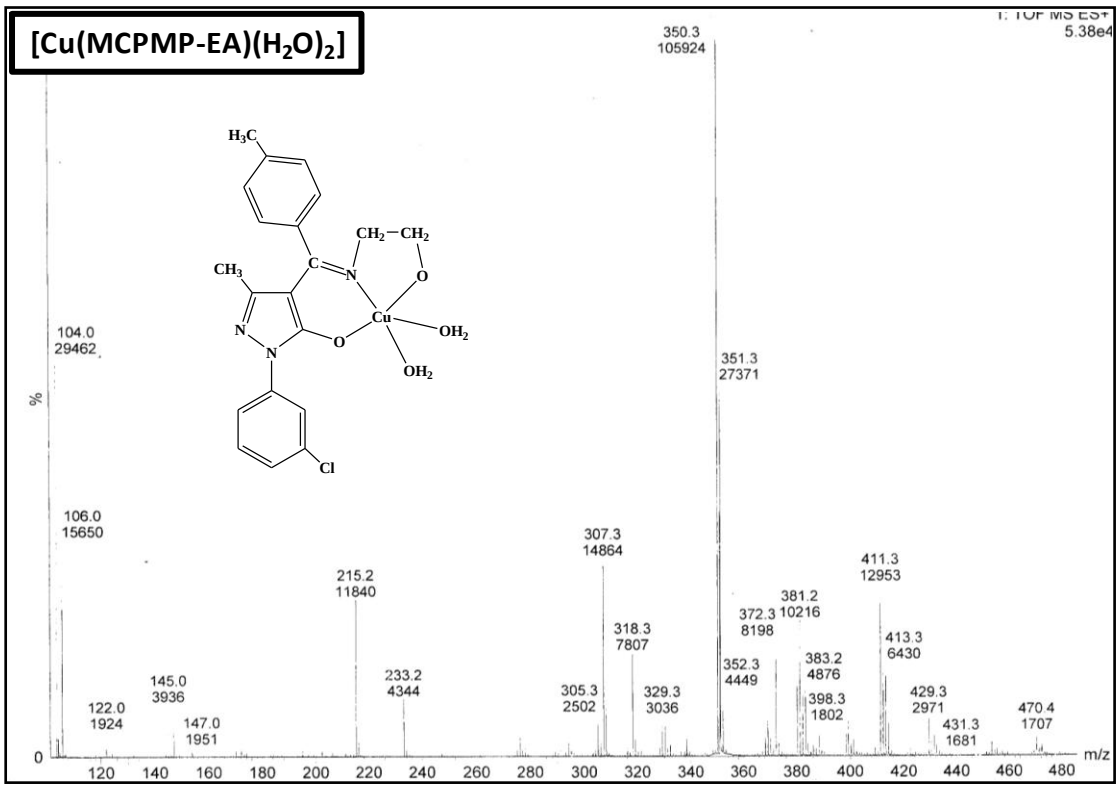

3.4.6 Thermal studies of the metal complexes

Thermal stability and thermal behavior of all complexes were studied by thermogravimetric analysis (TGA-DTA-DTG) at the atmosphere of nitrogen in the temperature range 25–700°C. The correlations between the different decomposition steps of the complexes with the corresponding weight losses are discussed in terms of the proposed formula of the complexes. The thermal behavior of all the complexes is almost same. The TGA profiles over the temperature range 30–300°C are usually due to loss of water of moisture, hydration and coordination. If the water molecules are of crystallization or lattice water molecules, it will be lost before 100°C. Here, in this case no mass loss was observed up to 240°C. The complexes have first decomposition stage in the range 250-310°C. This dehydration process probably is due to the loss of coordinated water molecules [273]. Above 300°C, complexes decompose in a gradual manner, which may be due to fragmentation and thermal degradation of the organic moiety. The continuous loss of weight is observed up to 700°C, respectively. This process is accompanied by exothermic process at around 300°C in DTA and DTG curves of the complexes. For these complexes, mass loss corresponds to loss of 8.31 % (Calc. 8.35 % for complex [Cu(PMP-EA)(H_2O)$_2$]), 7.24% (Calc. 7.20%, for complex [Cu(MCPMP-EA)(H2O)2]) and 8.05% (Calc. 8.08%, for complex

[Cu(PTPMP-EA)(H_2O)$_2$]) for two water molecules. Thus, there are two coordinated waters in all three complexes. (Figure 3.16-3.18)

Figure 3.16: TG DT analysis of metal complex [Cu(PMP-EA)(H_2O)$_2$]

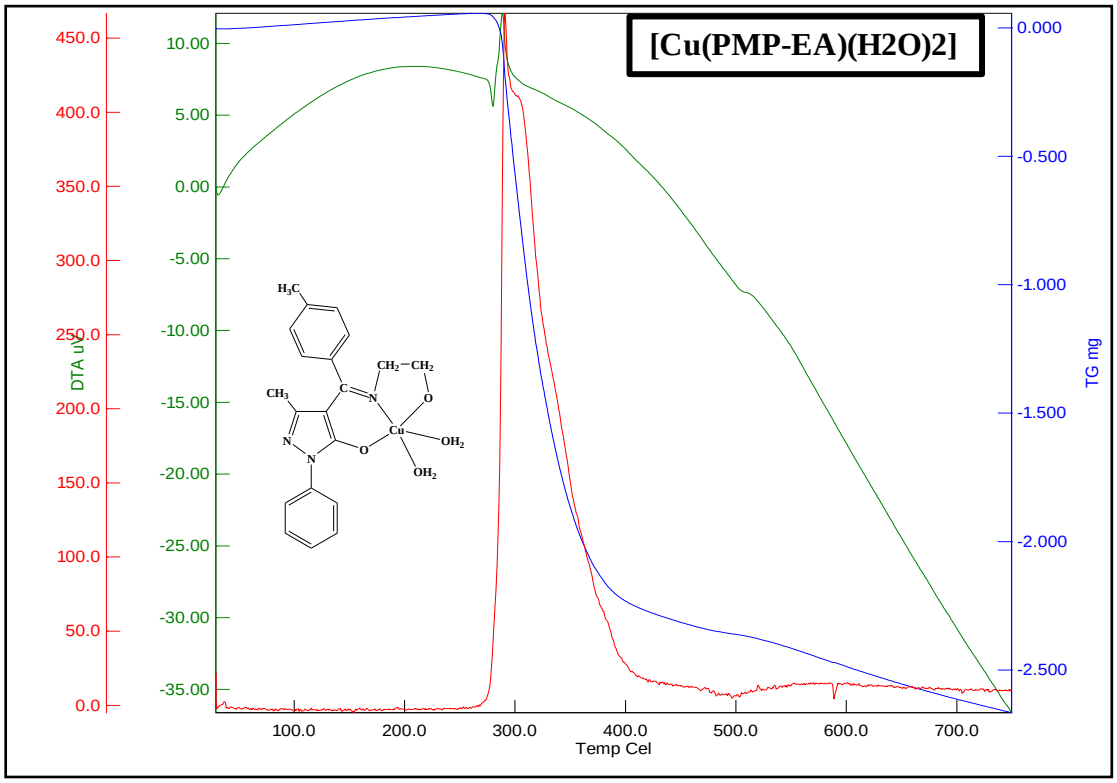

Figure 3.17: TG DT analysis of metal complex [Cu(MCPMP-EA)(H_2O)$_2$]

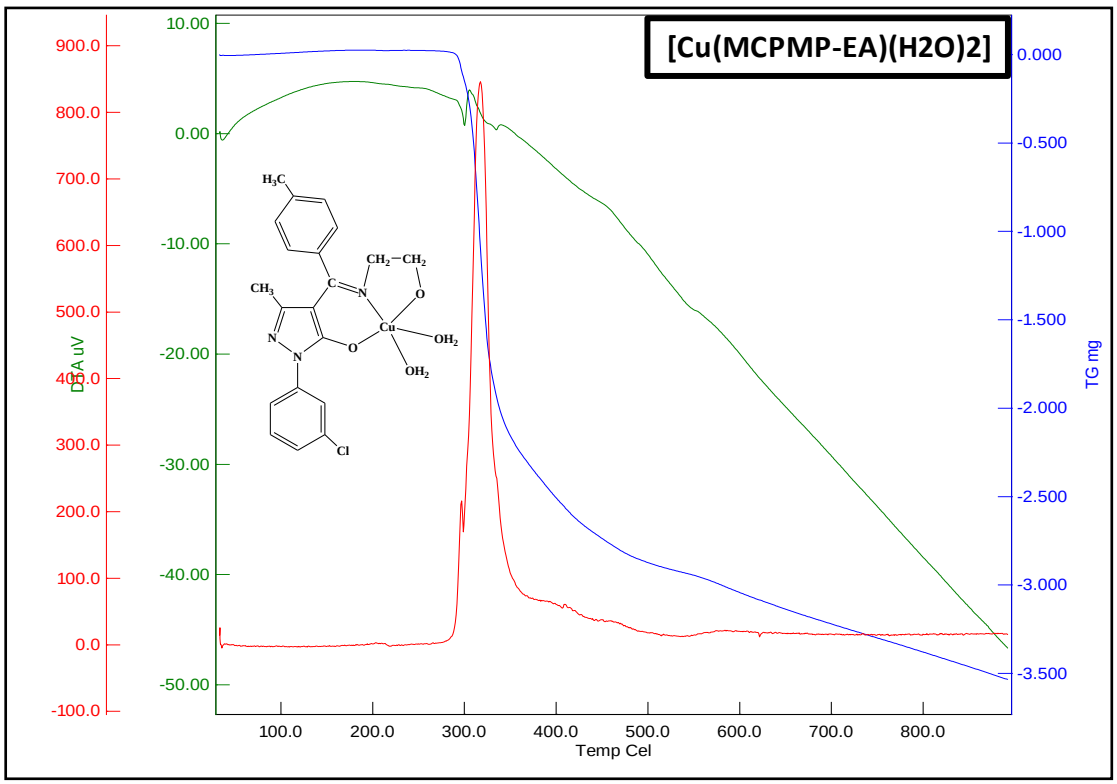

Figure 3.18: TG DT analysis of metal complex [Cu(PTPMP-EA)(H_2O)$_2$]

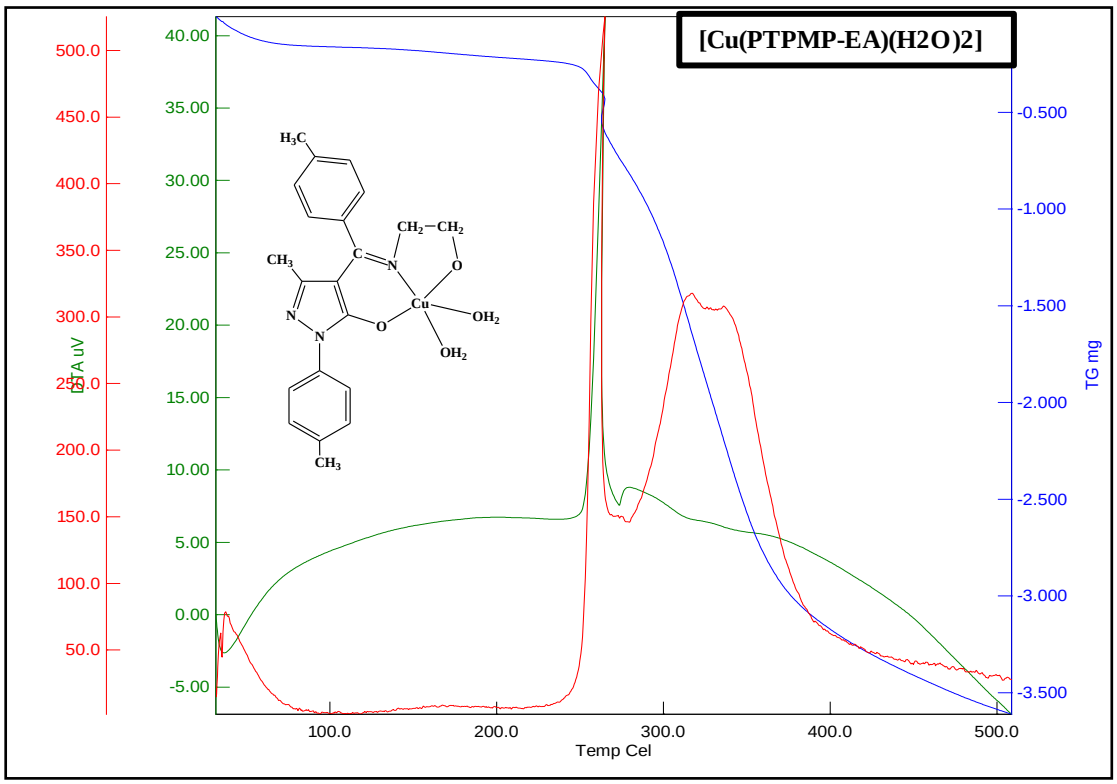

3.4.7 UV – Visible Spectral studies

Electronic spectra serve as a tool to distinguish between the square-planar, octahedral and tetrahedral geometries of the complexes. Electronic absorption of the complexes in the DMF solution shows a *d–d* transition in the range 550-660 nm, which can be assigned as the d_{xz}, $d_{yz} \rightarrow {}^2d_{x^2-y^2}$ transition, revealing that the Cu(II) is penta coordinated [202, 274-277].(Figure 3.19)

Figure 3.19: UV-Visible spectrum of [Cu(PTPMP-EA)(H_2O)$_2$]

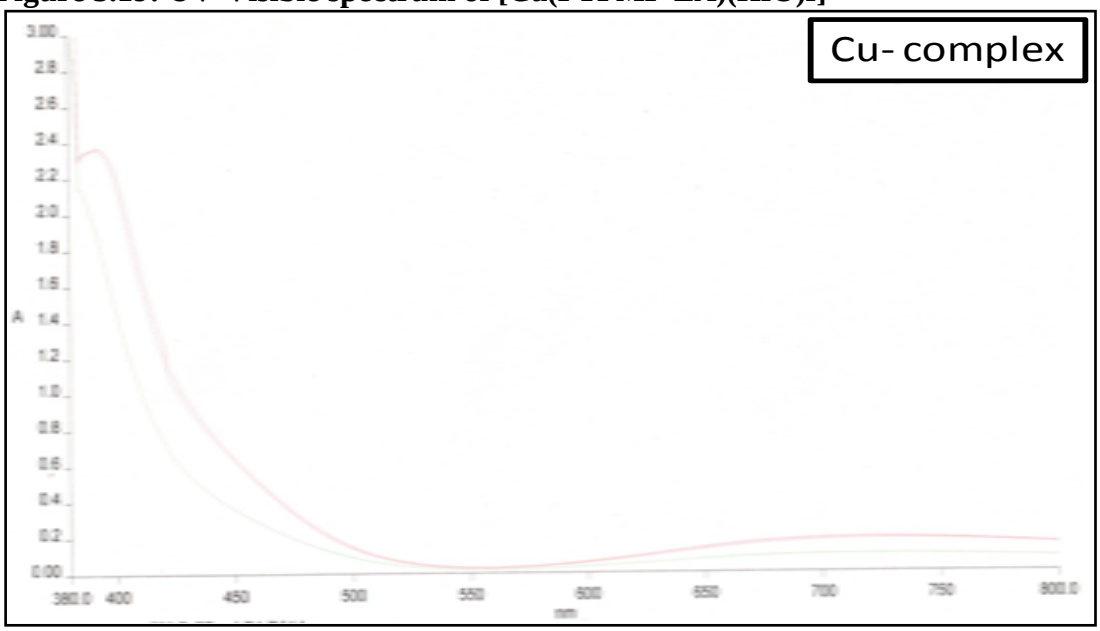

3.4.8 ESR Spectral Study

The X-band ESR spectra were recorded only for solution and powder samples for the complex **6** at RT and LNT to obtain further information about the stereochemistry and the site of the metal–ligand bonding and to determine the magnetic environment in the metal complexes. The ESR spectra of the complex **6** at RT and LNT are shown in Figs. 3.20 and 3.21, respectively. The ESR spectrum of complex **6** in solid state was recorded in quartz tube. Solution spectrum of this complex was recorded in DMF using capillary tube. The solution spectrum was recorded to confirm that the complex does not undergo structural change in solution.

The spectrum of the complex at 300 K shows one intense absorption band in the high field region and is isotropic due to dumpling motion of the molecules. Hamiltonian parameters $g_{\|}$, $g_{\perp}$, $A_{\|}$ and $A_{\perp}$were also calculated.

For G < 4.0, the ligand forming the Cu(II) complex is regarded as a strong field ligand and the local tetragonal axes are misaligned, and the unpaired electron is present in the d_{x2-y2} orbital and the exchange coupling effects are not operative in the present copper complex. For complex **6**, G = 2.13, indicating that the ligands are strong field ligands and the metal–ligand bonding in these complexes is covalent. It also indicates that the stereochemistry of complex is square pyramidal [278].

The orbital reduction factors ($K_{\|}$ and $K_{\perp}$) were also calculated.The observed values indicate that the complex has covalent character and in planeπ-bonding is also present in complex. In the case of pureσ- bonding $K_{\|}=K_{\perp}$,whereas $K_{\|}<K_{\perp}$ implies considerable in-planeπ-bonding while for out-plane π-bonding $K_{\|} > K_{\perp}$. For the present complex, the observed order is $K_{\|}$ (0.79) $>K_{\perp}$ (0.41) implyingagreatercontributionfromout-planeπ-bondingthanfromin-plane π-bonding in metal ligand π-bonding. Since there is no crystal structure determination of the complexes were done, from electronic and ESR spectral measurements we would like to safely assign square pyramidal geometry to these penta-coordinated copper complexes(Figure 3.20-3.21).

Figure 3.20: ESR spectrum of Cu-complex

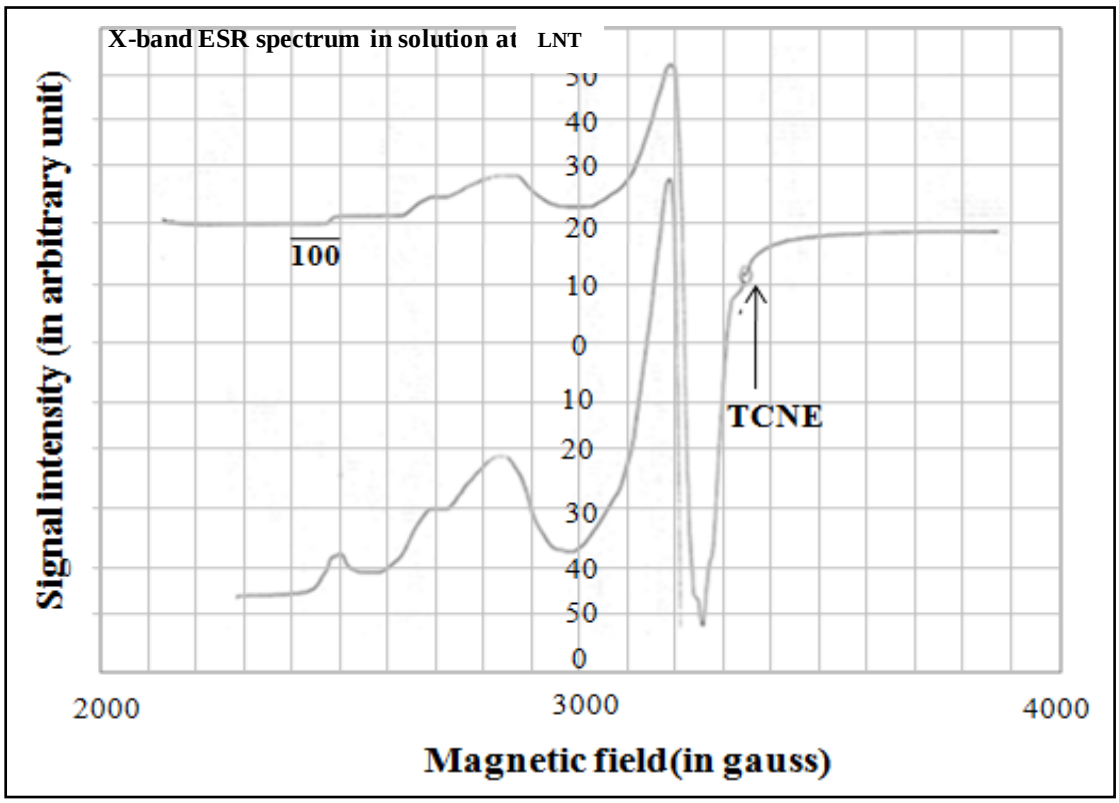

Figure 3.21: ESR spectrum of Cu-complex

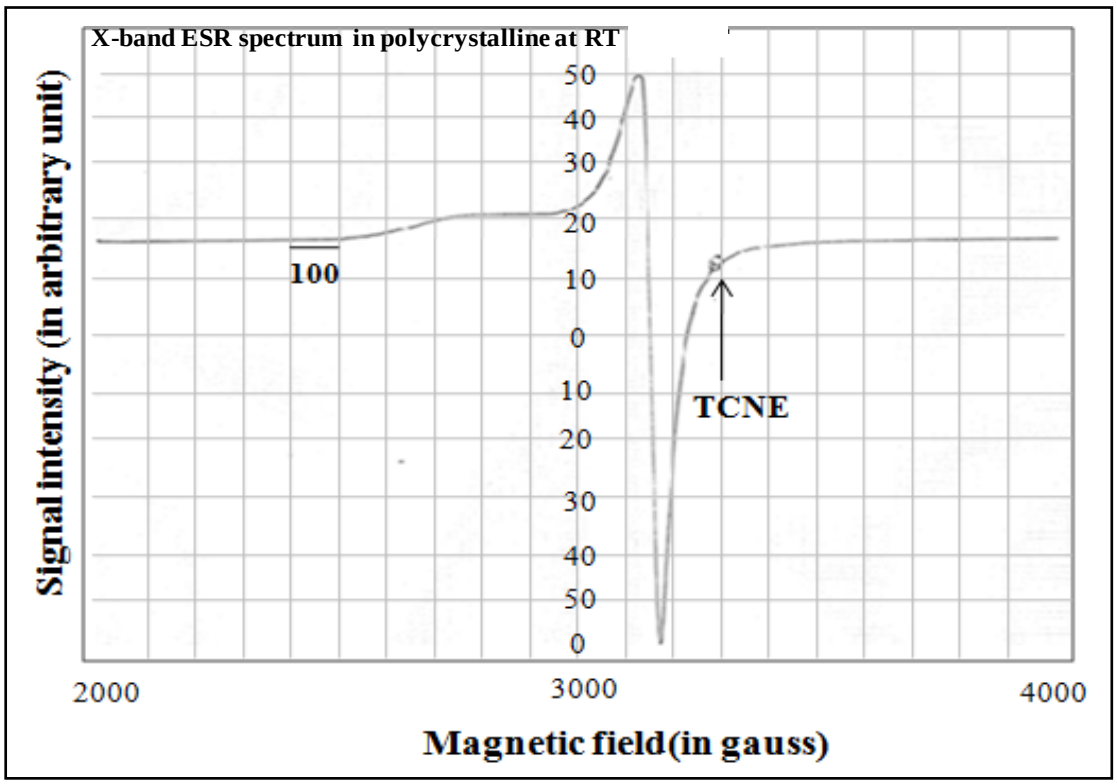

3.5DNA binding studies

3.5.1 Absorption spectral studies

The binding behavior of the metal complexes to DNA helix is often investigated using absorption spectral titration, followed by the changes in absorbance and shift in wavelength. Absorption spectral titration experiments were performed by maintaining a constant concentration of the complex and varying the nucleic acid/nucleotide concentration. This was achieved by diluting an appropriate amount of the metal complex solutions and CT-DNA stock solutions while maintaining the total volume constant. This results in a series of solutions with varying concentrations of CT-DNA but a constant concentration of the complex. The absorbance (A) was recorded after successive additions of CT-DNA.

With increasing concentration of CT-DNA, the absorption bands of the complexes were affected, resulting in the tendency of hypochromism and a slight red shift was observed in all the complexes due to the intercalative binding between DNA and metal complexes. Hyperchromic and hypochromic effects are the spectral features of DNA concerning its double helix structure. This spectral change showed that the change of DNA in its conformation and structure after the complex bound to DNA. Hypochromism results from the contraction of DNA in the helix axis, as well as from the change in conformation on DNA, while hyperchromism results from the damage of the DNA double helix structure. The absorption spectra of DNA in the absence and presence of complexes are given in figure 3.22. All the metal complexes showed decrease in absorption intensity (hypochromism) with a slight red shift which is due to the intercalative binding between DNA and metal complexes [279-282].

To further illustrate the DNA binding strength, the intrinsic binding constant K_b was determined by the standard given equation for the complexes, which were found to be 0.9×10^5 M^{-1}**(4)**, 1.2×10^5 M^{-1} **(5)** and 1.41×10^5 M^{-1} **(6)**. The binding constants of these complexes were lowerin comparison to those observed for typical classical intercalators (ethidium-DNA, 1.4×10^{6} M^{-1}) [283].The diminution of the intrinsic binding constants could be explained by the steric constraints imposed by the ligand framework and thus encouraging a partial intercalation calation binding mode for the complexes. Our results are consistent with earlier report sonpreferential binding to DNA intheCucomplexes[284,285].Plotsof [DNA]/ (ε_a-ε_f)versus [DNA] are shown in Fig. 3.23. From the values of binding constants, it can be concluded that the complex **6** has more binding affinity than other two complexes and the order of binding is **6**>**5**>**4.**

3.5.2Competitive DNA-binding studies with EB

The emission spectrum is obtained by setting the excitation monochromator at the maximum excitation wavelength and scanning with emission monochromator. Often an excitation spectrum is first made in order to confirm the identity of the substance and to select the optimum excitation wavelength. Further experiments were carried out to gain support for the mode of binding of complexes with CT-DNA. Non-fluorescent or weakly fluorescent compounds can often be reacted with strong fluorophores enabling them to be determined quantitatively. On this basis molecular fluorophore Ethidium bromide was used which emits fluorescence in presence of CT-DNA due to its strong intercalation. Quenching of the fluorescence of EB bound to DNA were measured with increasing amount of metal complexes as a second molecule.

In our experiments, as depicted in figure, the fluorescence intensity of EB show a remarkable decreasing trend with the increasing concentration of the complexes, indicating that some EB molecules are released from EB-DNA complex after an exchange with the complexes **4, 5 and 6** which result in the fluorescence quenching of EB. This may be due either to the metal complex competing with EB for the DNA-binding sites thus displacing the EB (whose fluorescence is enhanced upon DNA binding) or it should be a more direct quenching interaction on the DNA itself [321]. We assume the reduction of the emission intensity of EB on increasing the complex concentration could be caused due to the displacement of the DNA bound EB by the Cu(II) complexes. Such a quenched fluorescence behavior of EB bound to DNA caused by the interaction between the Cu(II) complexes and DNA is also found in other copper complexes [324,325]. Plot of relative fluorescence intensity (F_0/F) versus concentration for the complexes is shown in figure.

The Stern-Vormer constants were calculated for all the complexes using the Stern-Vormer equation. The constants found for the complexes are 1.26×10^7 M^{-1}, 1.30×10^7 M^{-1} and 1.31×10^7 M^{-1}. They are in good agreement with reported literature [286,287]. The values show that the complex **6** has higher binding capacity than the other two complexes.

3.5.3 Viscosity studies

The nature of binding of the complexes to the CT-DNA was further investigated by viscometric studies. The relative specific viscosity of DNA was determined by varying the concentration of the added metal complexes. Measuring the viscosity of DNA is a classical technique used to analyze the DNA binding mode in solution. In the absence of crystallographic structural data, hydrodynamic methods that are sensitive to DNA length change are regarded as the least ambiguous and the most critical tests of binding in solution. A classical intercalation model results in the lengthening of the DNA helix as the base pairs are separated to accommodate the binding molecule, leading to an increase in the DNA viscosity. However, a partial and/ or non-classical intercalation of ligand may bend (or kink) DNA helix, resulting in the decrease of its effective length and concomitantly its viscosity [282, 283, 288]. The plots of $(\eta/\eta o)^{1/3}$ vs. [Complex]/[DNA]=R (where η and ηo are the relative viscosities of DNA in the presence and absence of complex respectively) give a measure of the viscosity changes. The effects of all the complexes on the viscosity of CT DNA are shown in figure 3.26.

A significant increase in the viscosity of DNA on addition of complex results due to the intercalation which leads to the separation among the DNA bases to the increase in the effective size in DNA which could be the reason for the increase in the viscosity [289, 290]. The graph shows that the order of binding of the complexes is **6**>**5>4.** (Figure 3.22-3.26)

Figure 3.22: The Electronic spectra of the complexes 4 (A), 5 (B) and 6 (C) (1×10−3 M) in DMF in the absence and presence of CT-DNA. Arrow shows that the absorbance changes upon increasing DNA concentrations.

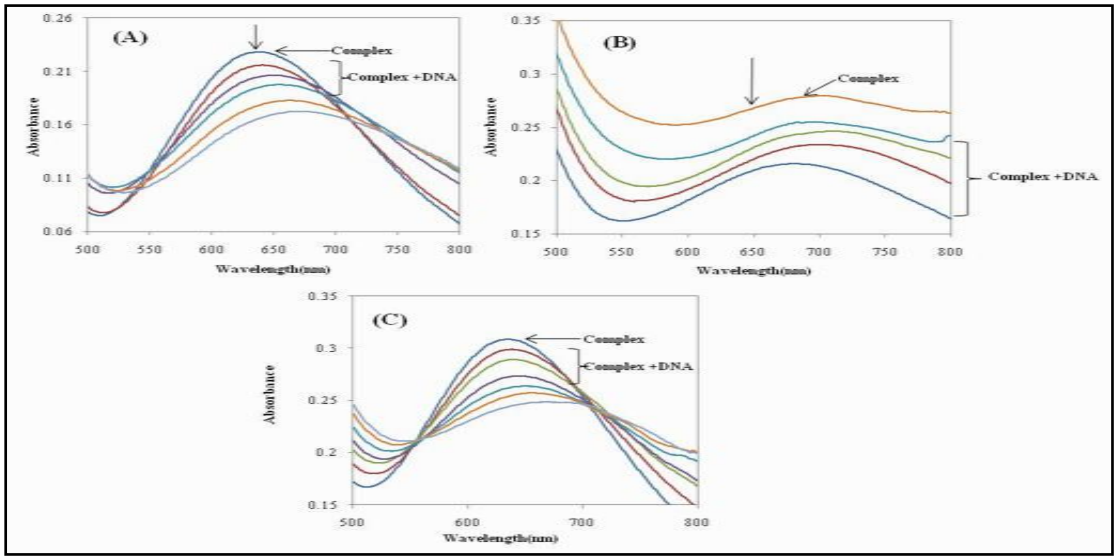

Figure 3.23: Plotsof [DNA]/ (ε_a-ε_f)versus [DNA]forthe titration ofDNAwithcomplexes 4 (A), 5 (B) and 6 (C).

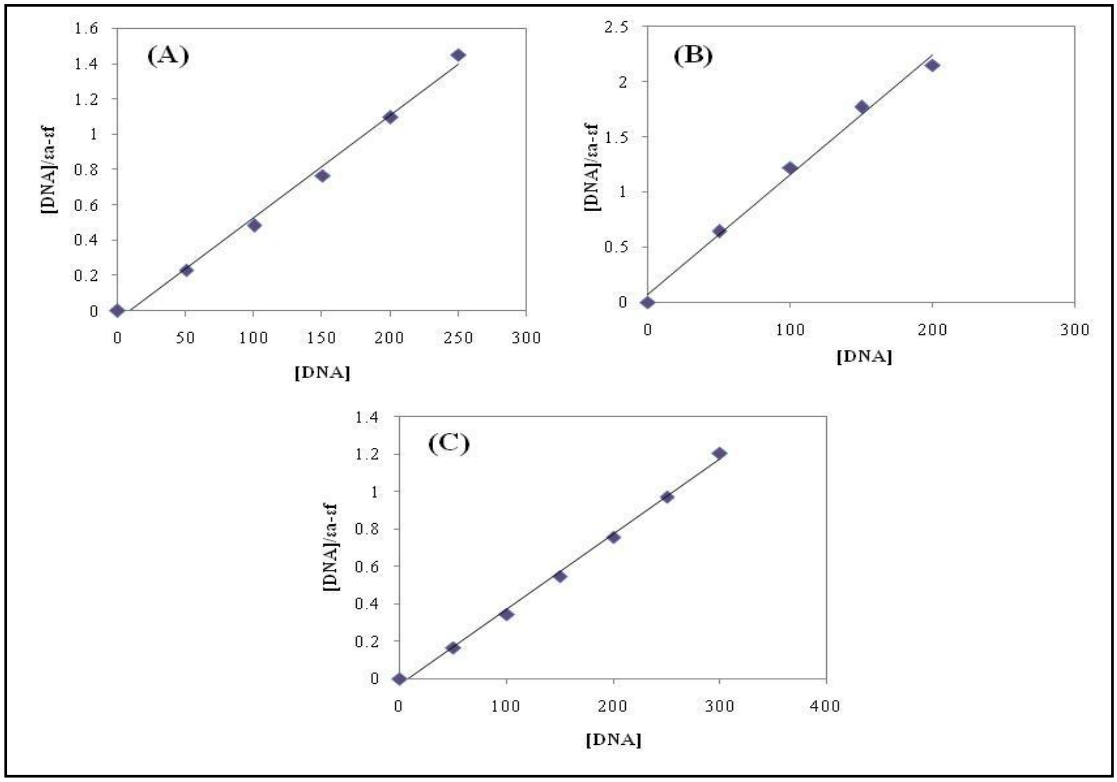

Figure 3.24: EmissionspectraofEB boundtoDNAin theabsenceandpresenceofcomplexes 4 (A), 5 (B) and 6 (C). [EB]=3.3µM,[DNA]=3µM; λ_{ex}=610nm.Thearrowshowstheintensitychanges on increasingthecomplexconcentration.

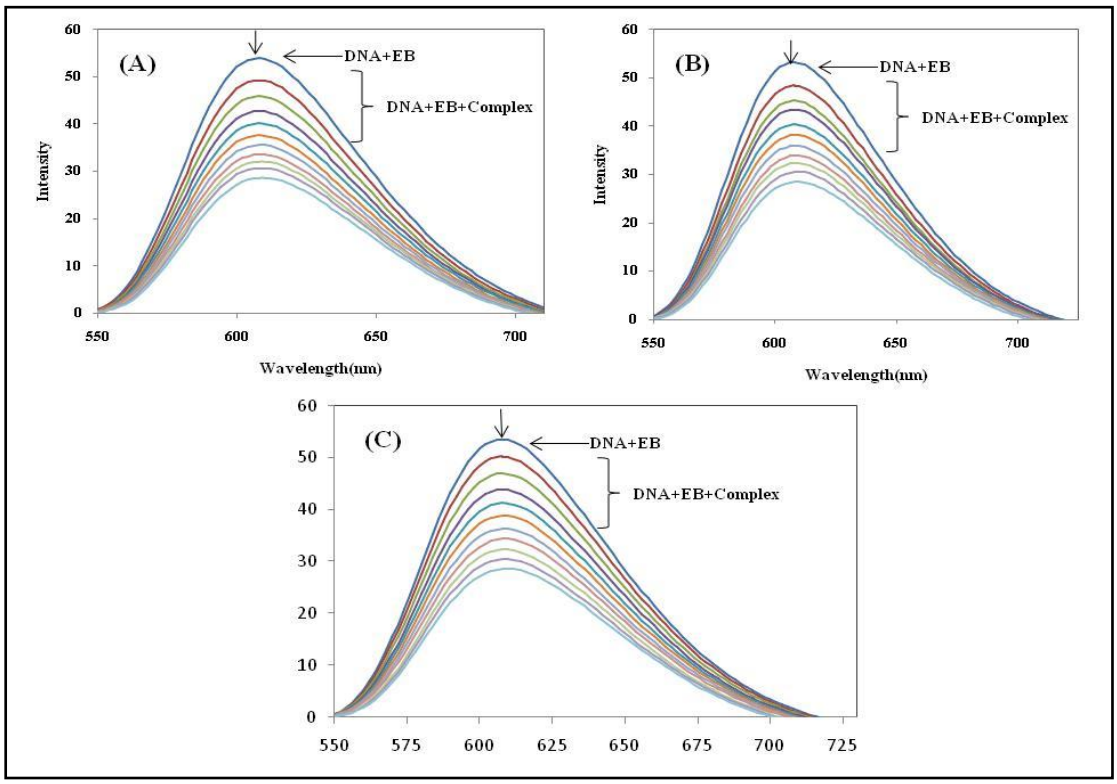

Figure 3.25: Plot of relative fluorescence intensity (F_0/F) versus concentration for the complexes 4-6 in buffer solution (150 mM NaCl and 15 mM trisodium citrate at pH 7.03) (λem = 546 nm)

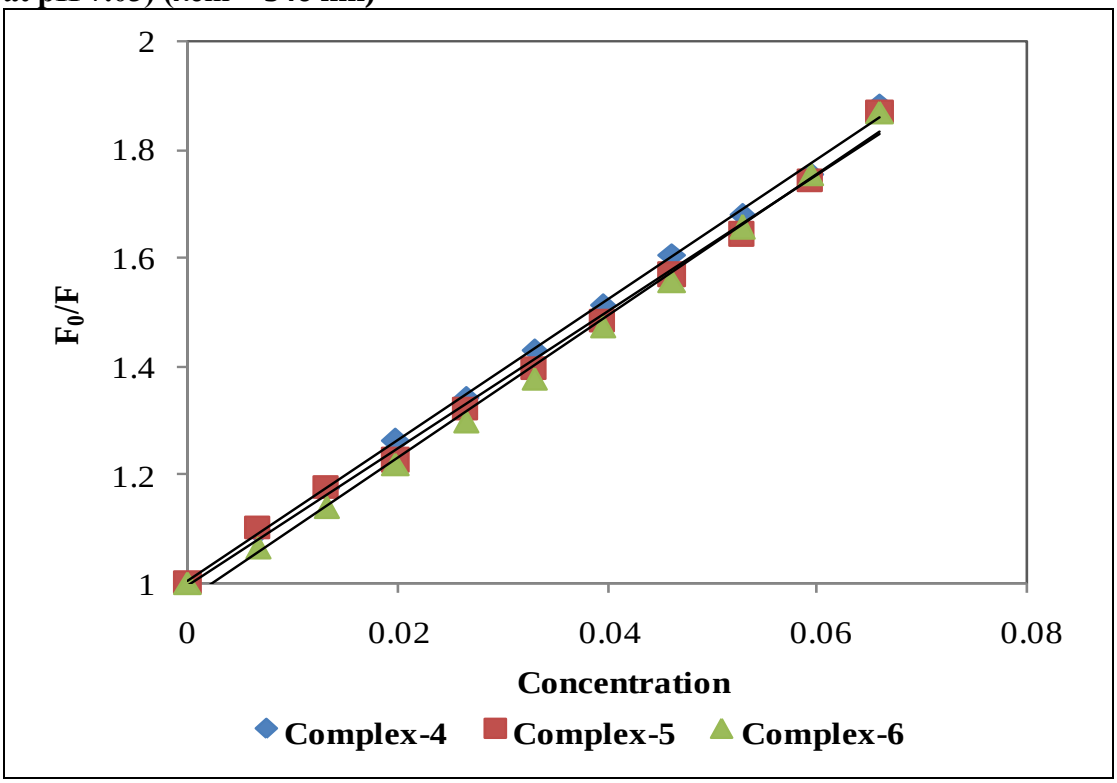

Figure 3.26: Effect of increasing amounts of complexes 4 (A), 5 (B) and 6 (C)on the relative viscosities of DNA at 30.0 ± 0.1 °C. [DNA] = 1 mM, [Complex]/[DNA] = 0, 0.01, 0.02, 0.03, 0.04, 0.05, 0.06, respectively.

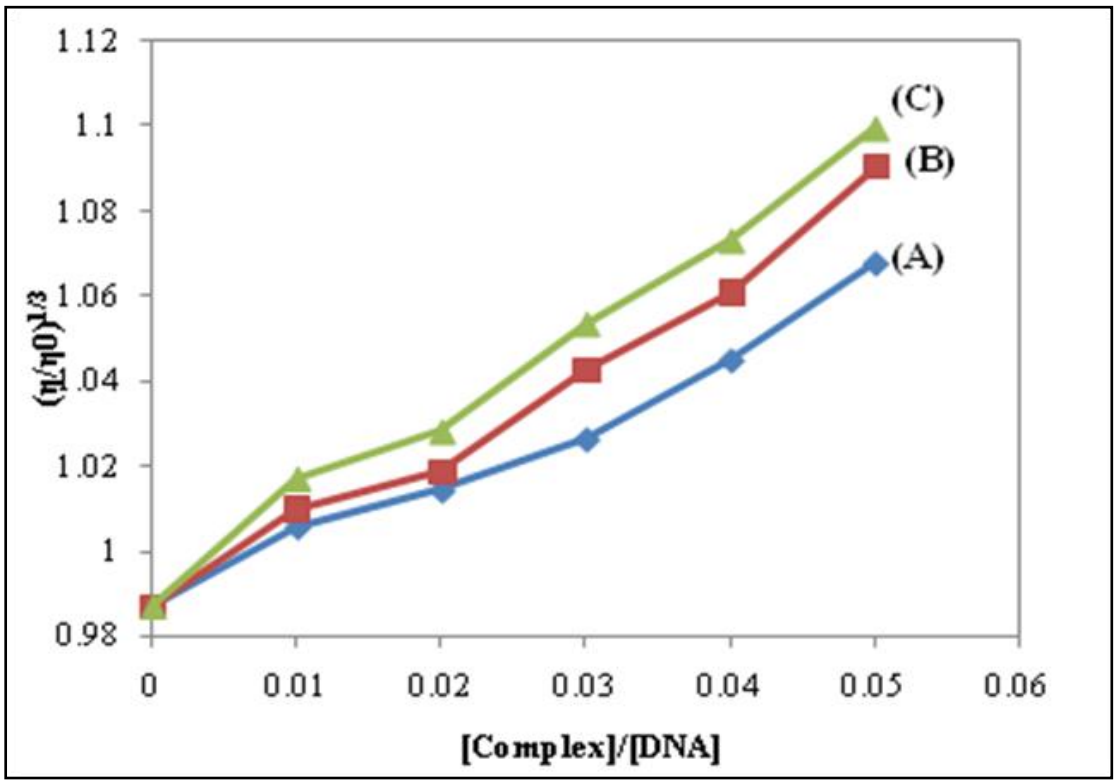

3.6 Conclusion

A series of Cu(II) complexes with Schiff base ligands derived from 4-toluoyl pyrazolones and 2-ethanolamine was synthesized and characterized. The spectral data show that all the Schiff bases exist as tridentate ligands by bonding to the Cu(II) ion through the deprotonated enol-O, deprotonated acidic-O and azomethine nitrogen. The analytical data show the presence of one Cu(II) per one ligand molecule and suggest a mononuclear structure for the complexes. The correlation of the experimental data allows assigning a square pyramidalstereochemistry to theabove synthesized complexes. The binding behavior of metal complexes with DNA was studied by UV spectra, viscosity and fluorescence assay under physiological conditions. All the experimental evidences indicate that these complexes can strongly bind to CT-DNA *via* an intercalation mode. Among the three complexes, complex 6 has higher binding affinity than other two complexes. Results obtained from our present work would be very useful to understand the mechanism of interactions of the small molecules binding to DNA and helpful in the development of their potential applications in biological, pharmaceutical and physiological fields in future.

3.7 References

240. G.F. de Sa, O.L. Malta, C. de Mello Donega, A.M. Simas, R.L. Longo, P.A. Santa-Cruz, E.F. da Silva Jr., Coordination Chemistry Reviews, 196 (2000) 165 – 195

241. M. D. McGehee, T. Bergstedt, C. Zhang, A. P. Saab,M. B. O'Regan, G. C. Bazan, V. I. Srdanov, A. J. Heeger, Advanced Materials, 11(16) (1999) 1349–1354.

242. M. Elbanowski, B. Makowska, K. Staninski, M. Kaczmarek,Journal Photochemical and Photobiology A,130(2-3) (2000) 75-81.

243. G. Vicentini, L.B. Zinner, J. Zukerman-Schpector, K. Zinner, Coordination Chemistry Reviews, 196(1) (2000) 353-382.

244. Piotr Dobrzynski, Janusz Kasperczyk, Maciej Bero, Macromolecules, 32(14) (2000) 4735–4737.

245. Maciej Bero, Piotr Dobrzynski, Janusz Kasperczyk, Polymer Bulletin, 42(2) (1999) 131-139.

246. B.K.Keppler, C. Friesen, H. Vongerichten, E. Vogel In: Keppler BK (ed) Metal complexes in cancer chemotherapy. VCH, Weinheim,(1993) 297–323.

247. D. Sil, R. Kumar, A.Sharon, P.R.Maulik, V.Ji Rama, Tetrahedron Letters, 46 (2005)3807–3809.

248. A.Tanitame, Y.Oyamada, K.Ofugi, M.Fujimoto, N.Iwai, Y.Hiyama, K.Suzuki, H.Ito, H.Terauchi, M.Kawasaki, K.Nagai,M.Wachi, J. Yamagishi, Journal of Medical Chemistry, 47 (2004)3693.

249. P. Chiba, W. Holzer, M.Landau, G. Bechmann, K. Lorenz, B. Plagens, M.Hitzler, E.Richter, G.Ecker,Journal of Medical Chemistry, 41 (1998) 4001.

250. R.N. Jadeja, J.R. Shah, E. Suresh, P. Paul, Polyhedron, 23 (2004) 2465

251. I.A. Patel, P. Patel, S. Goldsmith, B.T. Thaker, Indian Journal of Chemistry, 42A (2003)2487.

252. R.C. Maurya, M.N. Jayaswal, D.D.Mishra, S.Kovil,Synthesis and Reactivity in Inorganic, Metal-Organic and Nano-Metal Chemistry,27 (1997)49.

253. I.A.Patel, B.T. ThakerIndian Journal of Chemistry, 38 (1999)427

254. R.N. Jadeja, R.N. Shirsat, E. Suresh, Structural Chemistry, 16(5)(2005)515.

255. R.J.Yadav, K.M. Vyas, R.N.Jadeja,Journal of Coordination Chemistry,63(10) (2010).

256. R.N.Jadeja and J.R. Shah, Polyhedron, 26 (2007) 1667.

257. N.J. Parmar and S.B. Teraiya, Journal of Coordination Chemistry 62(14) (2007) 2388-2398.

258. S. Parihar, S. Pathan, R.N. Jadeja, A. Patel, V.K. Gupta, Inorganic chemistry 51(2) (2012) 1152-1161.

259. N. P. Moorjani, K. M. Vyas, and R. N. Jadeja, Journal of Pure and Applied Sciences, 18(2010) 68–72.

260. R.N. Jadeja, Mitesh Chhatrola, V. K. Gupta, Polyhedron, 63 (2013) 117–126.

261. R.N.Jadeja, S. Parihar, K. Vyas, V.K. Gupta,Journal of Molecular Structure, 1013 (2012) 86-94.

262. K.M.Vyas, R.N.Jadeja,D. Patel, R.V.Devkar,V.K.Gupta,Polyhedron,65, (2013) 262-274.

263. J.Marmur,Journal of Molecular Biology,211(1961) 3208.

264. M.E. Reichman, S.A. Rice, C.A. Thomas, P. Doty,Journalof American ChemistrySociety, 76 (1954)3047.

265. R.N. Jadeja, K.M. Vyas, V.K. Gupta, R.G. Joshi, C. Ratna Prabha. Polyhedron, 31 (2012)767.

266. L. J. Farrugia,Journal of AppliedCrystallography, 30 (1997) 565.

267. D. Sinha, A.K. Tiwari, S. Singh, G. Shukla, P. Mishra, H. Chandra, A.K. Mishra. European Journal of Medicinal Chemistry, 43 (2008) 160.

268. B. T. Thaker, K. R. Surati, S. Oswal, R. N. Jadeja, V. K. Gupta,Structural Chemistry, 18 (2007) 295.

269. L.D. Popov, S.I. Levchenkov, I.N. Shcherbakov, V.V. Lukov, K.Y. Suponitsky, V. Kogan,Inorganic Chemistry Communication, 17 (2012) 1-4.

270. N. Parmar, S. Teraiya, R. Patel, H. Barad, H. Jadeja, V. Thakkar,Journal of Saudi Chemical Society, (2011) 10-15.

271. R.N. Jadeja, S. Parihar, K. Vyas, V.K.Gupta,Journal of Molecular Structure,1013 (2012) 86-94.

272. V.F. Shulgin, O.V. Konnik, S.V. Abkhairova, Inorganica Chimica Acta,402(100) (2013) 33-38.

273. C. K. Modi, M. N. Patel, Journal of Thermal Analysis and Calorimetry, 94(2008)247.

274. F. A. Mautner, C. N. Landry, A. A. Gallo, S. S. Massoud, Journal of Molecular Structure,837 (2007)72.

275. B. J. Hathaway, Journal of Chemical Society, Dalton Trans. 1 (1972) 1196.

276. B. J. Hathaway, G. Wilkinson, R.D. Gillard, J.A. McCleverty (Eds.), Comprehensive Coordination Chemistry, Pergamon Press, Oxford, UK,5, (1987) 533.

277. U. Mukhopadhyay, I. Bernal, S. S. Massoud, F. A. Mautner, Inorganica Chimica Acta, 357, (2004) 3673.

278. P. UmaMaheswari,M. Palaniandavar,InorganicaChimica Acta., 357(2004)901.

279. A. Colak, U. Terzi, M. Col, S.A. Karaoglu, S. Karabocek, A. Kucukdumlu, F.A. Ayaz. European Journal of Medicinal Chemistry, 45 (2010)5169.

280. S.H Cui, M. Jiang, Y.T. Li, Z.Y. Wu, X.W. Li, Journal of Coordination Chemistry, 64 (2011)4209.

281. N. Raman, K. Pothiraj, T. Baskaran, Journal of Coordination Chemistry, 64(2011)4286.

282. Y. Mei, J.J. Zhou, H. Zhou, Z.Q. Pan, Journal of Coordination Chemistry, 65 (2012)643.

283. J.B. LePecq, C. Paoletti,Journal of MolecularBiology, 27 (1967)87.

284. F. Arjmand, M. Aziz, EuropeanJournal of Medicinal Chemistry, 44(2009)834.

285. N. Raman,R. Jeyamurugan,A. Sakthivel,L. Mitu.Spectrochim.Acta.PartA., 75, 88 (2010).

286. U. McDonnell, M.R. Hicks, M.J. Hannon, A. Rodger,Journal of Inorganic Biochemistry, 102 (2008)2052.

287. M. Shakir, S. Khanam, M. Azam, M. Aatif, F. Firdaus, Journal of Coordination Chemistry, 64(2011) 3158.

288. S. Sathyanarayana, J.C. Dabroniak, J.B. Chaires, Biochemistry, 31 (1992) 9319.

289. S. Satyanarayana, J.C. Dabrowiak, J.B. Chaires, Biochemistry, 32 (1993)2573.

290. N. Raman, K. Pothiraj, T. Baskaran, Journal of Coordination Chemistry, 64 (2011) 3900.